RNAi-based screen for pigmentation in *Drosophila melanogaster* reveals regulators of brain dopamine and sleep

Samantha L Deal[1,2,#], Danqing Bei[2,3], Shelley B Gibson[2,3], Harim Delgado-Seo[2,4], Yoko Fujita[2,3], Kyla Wilwayco[2,3], Elaine S Seto[5,6,7], Shinya Yamamoto[1,2,3,4,8,*]

[1] Program in Developmental Biology, Baylor College of Medicine (BCM), Houston, TX 77030, USA

[2] Jan and Dan Duncan Neurological Research Institute (NRI), Texas Children's Hospital (TCH), Houston, TX 77030, USA

[3] Department of Molecular and Human Genetics, BCM, Houston, TX 77030, USA

[4] Department of Neuroscience, BCM, Houston, TX 77030 USA

[5] Department of Neurology, TCH, Houston, TX 77030, USA

[6] Epilepsy Center, TCH, Houston, TX 77030, USA

[7] Department of Neurophysiology, TCH, Houston, TX 77030, USA

[8] Development, Disease Models & Therapeutics Graduate Program, BCM, Houston, TX 77030, USA

[#]Current Address: Department of Neuroscience, University of Pennsylvania, Philadelphia, Pennsylvania, USA

*Corresponding Author: Shinya Yamamoto

Correspondence: yamamoto@bcm.edu

Summary

The dopaminergic system has been extensively studied for its role in behavior in animals as well as human neuropsychiatric and neurological diseases. However, we still know little about how dopamine levels are tightly regulated *in vivo*. To identify novel regulators of dopamine, we utilized *Drosophila melanogaster* cuticle pigmentation as a readout, where dopamine is a precursor to melanin. We measured dopamine from genes known to be critical for cuticle pigmentation and performed an RNAi-based screen to identify new regulators of pigmentation. We found 153 potential pigmentation genes, which were enriched for conserved homologs and disease-associated genes as well as developmental signaling pathways and mitochondria-associated proteins. From 35 prioritized candidates, we found 10 caused significant reduction in head dopamine levels and one caused an increase. Two genes, *clueless* and *mask (multiple ankyrin repeats single KH domain),* upon knockdown, reduced dopamine levels in the brain. Further examination suggests that Mask regulates the transcription of the rate-limiting dopamine synthesis enzyme, *tyrosine hydroxylase*, and its knockdown causes dopamine-dependent sleep phenotypes. In summary, by studying genes that affect cuticle pigmentation, a phenotype seemingly unrelated to the nervous system, we were able to identify several genes that affect dopamine metabolism as well as a novel regulator of behavior.

Keywords: *Drosophila melanogaster*, dopamine, pigmentation, RNAi, screen, *mask*, sleep

Introduction

Dopamine is a conserved neurotransmitter that functions in the nervous system to regulate a variety of behaviors, including learning & memory, locomotion, reward, and sleep. In humans, disruptions in dopamine have been associated with neurological and neuropsychiatric disorders, including addiction, depression, sleep disorders, and schizophrenia(1–3). In addition, one of the hallmarks of Parkinson's disease is early degeneration of dopaminergic neurons, and Parkinson's patients are often given a dopamine precursor, l-dihydroxyphenylalanine (L-DOPA), as a method for treating symptoms (4,5). Most genetic research on dopamine biology has focused on dopaminergic signaling and transport; however, changes in dopamine levels can have a great impact on behavioral outcomes (6–8). Thus, identifying genes that affect dopamine levels is critical to understanding and potentially treating dopamine-associated disorders.

Dopamine synthesis is a conserved process, whereby the amino acid tyrosine is converted into L-DOPA via the rate-limiting enzyme, Tyrosine hydroxylase (TH) (9). Then, L-DOPA is converted into dopamine via the enzyme Dopa decarboxylase (Ddc) (10). In mammals, dopamine is degraded via oxidation or methylation using the enzymes Monoamine oxidase (MAO) and Catechol-O-methyltransferase (COMT), respectively (11). In invertebrates, dopamine degradation goes through β-alanylation via the β-alanyl amine synthase (encoded by the *ebony* gene in *Drosophila melanogaster*) and acetylation via the acetyltransferase (encoded by the *speck* gene in *Drosophila*) (12). However, insects also convert dopamine into melanin to form proper cuticle pigment and structure. In fact, changes in genes that are involved in dopamine metabolism also change the cuticle color (13–15). In other words, knockdown of *TH* (or the *pale (ple)* in *Drosophila*) or *Ddc* leads to a paler cuticle, and mutations or knockdown of *ebony* or *speck* leads to a darker cuticle.

66 Historically, *Drosophila* has been used to study dopamine biology in multiple contexts,
67 including learning and memory (16,17). Over the years, an extensive genetic toolkit has been
68 generated in the fruit fly, making it a great system for dissecting dopaminergic neural circuitry and
69 signaling (18–20). In addition to the fly's contribution to understanding dopaminergic circuitry, this
70 model organism helped to identify and investigate the cellular functions of Parkinson disease's
71 genetic risk factors, *PINK1* and *PRKN* (i.e. *Pink1* and *parkin* in the fruit fly) (21). The conservation
72 of systems in neural biology along with the efficiency of working in *Drosophila* has made it a great
73 system for large-scale screening of novel genes. Previously, a large-scale RNAi screen (11,619
74 genes, ~89% of genome) was performed to identify genes that affect mechanosensory organs
75 and cuticle formation in the *Drosophila* thorax (22). In this screen, the researchers found 458
76 genes that affected cuticle color upon knockdown, but no further validation was performed.

77 Here, we utilize the fruit fly cuticle to identify novel regulators of dopamine. We start by
78 systematically examining classical pigmentation genes for their effect on dopamine in the head
79 and brain. From this we found that genes that are involved in dopamine synthesis are the only
80 genes with expected effects on dopamine; genes involved in degradation of dopamine either have
81 no effect or unexpectedly show reduced dopamine. We go on to characterize 458 genes identified
82 from the RNAi screen by Mummery-Widmer et al. (2009). We tested 330 of them with independent
83 RNAi lines and found 153 genes (~46%) with consistent cuticle pigmentation defects. We
84 examine 34 prioritized genes hits for changes in dopamine in the head and brain. From this
85 analysis, we found two genes, *mask* and *clu*, that reduced brain dopamine levels upon knockdown
86 in dopaminergic neurons. Lastly, we used molecular biology and sleep behavioral studies to show
87 that *mask* appears to alter brain dopamine through regulation of TH transcription.

88 # Results

Drosophila pigmentation genes affect dopamine in unexpected ways

To systematically test if changes in pigmentation genes affect dopamine as theorized in the field, we characterized loss-of-function alleles of genes involved in dopamine metabolism (Fig 1A) for pigmentation phenotypes and dopamine levels in the head and brain. The enzymes required for dopamine synthesis, TH and Ddc, are essential for survival (23,24). Thus, we took advantage of established RNAi lines and UAS/GAL4 system (25–28). It is known that reduction of *TH* or *Ddc* level or activity causes pale pigmentation and reduced dopamine (9,10,14). We validated our method by knocking down *TH* using a verified UAS-RNAi (29), which causes a strong pale cuticle phenotype (Figs 1B and 1-C), reduction in head dopamine by ~60% (Fig 1E), and reduction in brain dopamine by ~32% (Fig 1E'). *Ddc* knockdown causes a weaker effect than *TH* RNAi in the cuticle (Figs 1B and 1,D) and in the head (~35% dopamine reduction, Fig 1E), with no significant effect on dopamine in the brain (Fig 1E'). This may be due to the strength of the RNAi and/or enzyme level requirements (since TH is the rate-limiting enzyme).

Figure 1

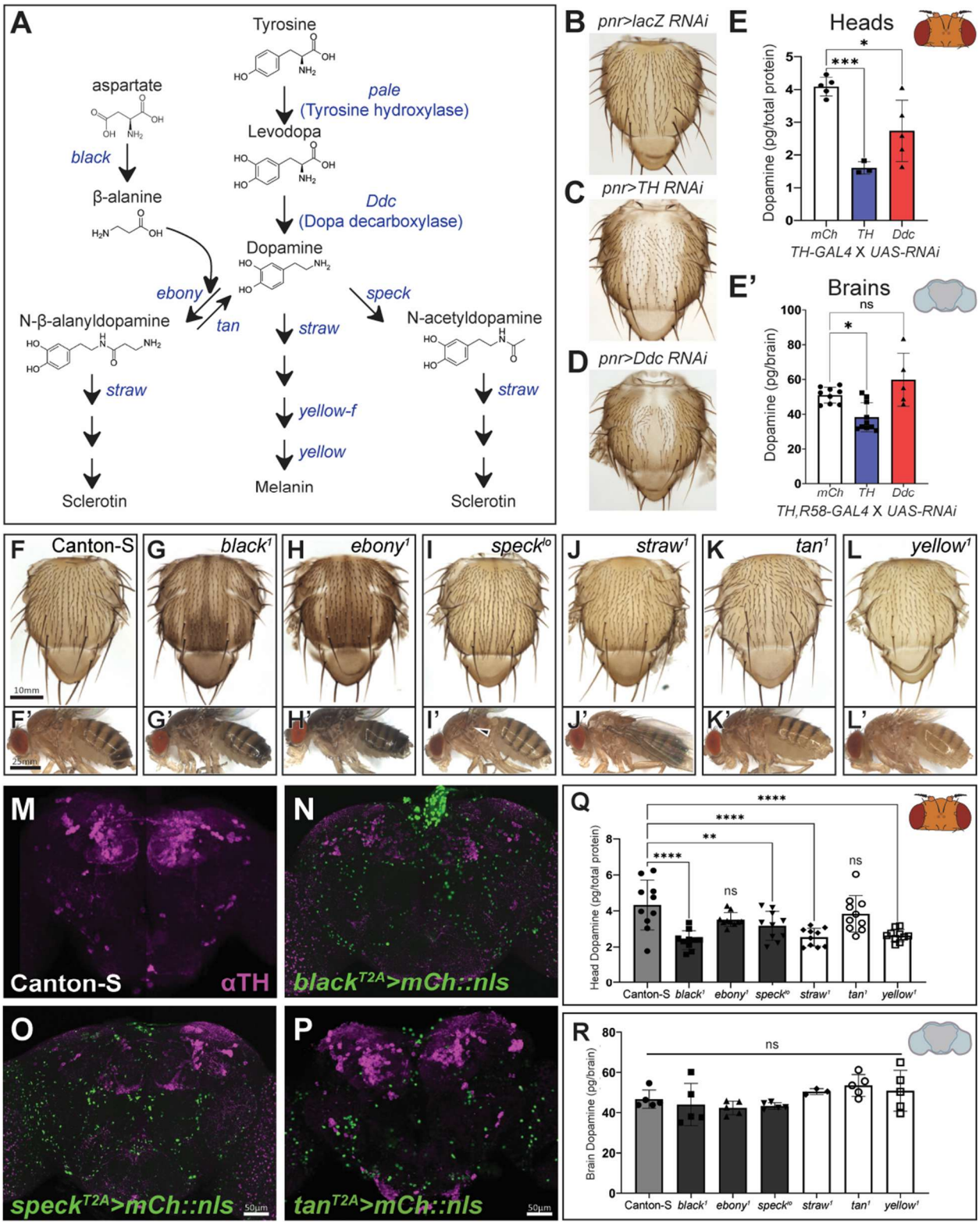
A
Tyrosine
aspartate
pale
(Tyrosine hydroxylase)
Levodopa
black
β-alanine
Ddc
(Dopa decarboxylase)
Dopamine
ebony
tan
speck
N-β-alanyldopamine
straw
N-acetyldopamine
straw
straw
yellow-f
yellow
Sclerotin
Melanin
Sclerotin
B pnr>lacZ RNAi
C pnr>TH RNAi
D pnr>Ddc RNAi
E Heads
Dopamine (pg/total protein)
mCh TH Ddc
TH-GAL4 X UAS-RNAi
E' Brains
Dopamine (pg/brain)
mCh TH Ddc
TH,R58-GAL4 X UAS-RNAi
F Canton-S
G black1
H ebony1
I speckl0
J straw1
K tan1
L yellow1
10mm
F' G' H' I' J' K' L'
25mm
M
Canton-S αTH
N
blackT2A>mCh::nls
O
speckT2A>mCh::nls
50µm
P
tanT2A>mCh::nls
50µm
Q
Head Dopamine (pg/total protein)
Canton-S black1 ebony1 speckl0 straw1 tan1 yellow1
R
Brain Dopamine (pg/brain)
Canton-S black1 ebony1 speckl0 straw1 tan1 yellow1

105 **Fig 1. Manipulation of pigmentation enzymes have unexpected effects on dopamine.** (A)
106 *Drosophila* dopamine metabolism pathway. Gene names encoding pigmentation enzymes are in
107 blue and metabolites are in black. (B-D) Thorax phenotypes observed upon knockdown of
108 Tyrosine hydroxylase (TH, also known as Pale) (C) and Dopa decarboxylase (Ddc) (D) compared
109 to control (B). (E-E') Dopamine levels from the head (E) and brain (E') upon knockdown of *TH*
110 and *Ddc*. Pigmentation phenotypes observed mutant alleles in the thorax (F-L) and the body (F'-
111 L') (Arrow in I' indicates the darker region characteristic of *speck* mutants). *T2A-GAL4* alleles for
112 *black*, *speck*, and *tan* adult brain expression with dopaminergic neurons (DAN) staining in
113 magenta (DANs) (M-P). (Q) Dopamine in the head of classical pigmentation mutants, $black^1$,
114 $ebony^1$, $straw^1$, and $yellow^1$. (R) Dopamine levels in dissected brains of classical pigmentation
115 mutants. Ordinary one-way ANOVA test with Dunlett multiple comparisons test. *=p<0.05,
116 **=p<0.01, ***=p<0.001, ****=p<0.0001. Error bars show standard deviation (SD).

117

118

119 To test genes implicated in dopamine degradation and cuticle development (pigmentation
120 and structural rigidity), we examined known mutant alleles. These alleles cause darker or paler
121 cuticles (Figs 1F-1L and, 1F'-1L') depending on their role in melanin metabolism. Unexpectedly,
122 *black*, *speck*, *straw* and *yellow* mutants reduce head dopamine levels (Fig 1Q), while *ebony* and
123 *tan* mutants had no significant effect (Fig 1Q). Next, we checked the brain expression patterns of
124 pigmentation enzymes. Based on our own expression analysis (Figs 1M-1P) and previously
125 reported expression data (30,31), most are expressed in the fly brain, but their expression does
126 not appear to overlap with DANs. However, we found no significant effect on brain dopamine in
127 these pigmentation genes (Fig 1R).

128 Together this data shows that changes in dopamine synthesis cause a paler cuticle, which
129 reflects a reduction in dopamine, but changes in dopamine metabolism enzymes downstream of
130 dopamine synthesis have pigmentation phenotypes that do not correlate with dopamine level
131 differences.

132 RNAi-based cuticle pigmentation screen

133 Mining a previously published genome-wide scale RNAi screen (22), we identified 458
134 genes with pigmentation defects. To check if these phenotypes can be reproduced, we located
135 718 additional UAS-RNAi lines corresponding to 330 genes. 426 lines came from the National
136 Institute of Genetics in Mishima, Japan (32), and 292 came from the Transgenic RNAi Project
137 (TRiP) at Harvard Medical School (25). 153 genes caused pigmentation defects in at least one
138 additional RNAi line, showing a validation of 46.4% from the previous screen (Fig 2A).

139

Figure 2

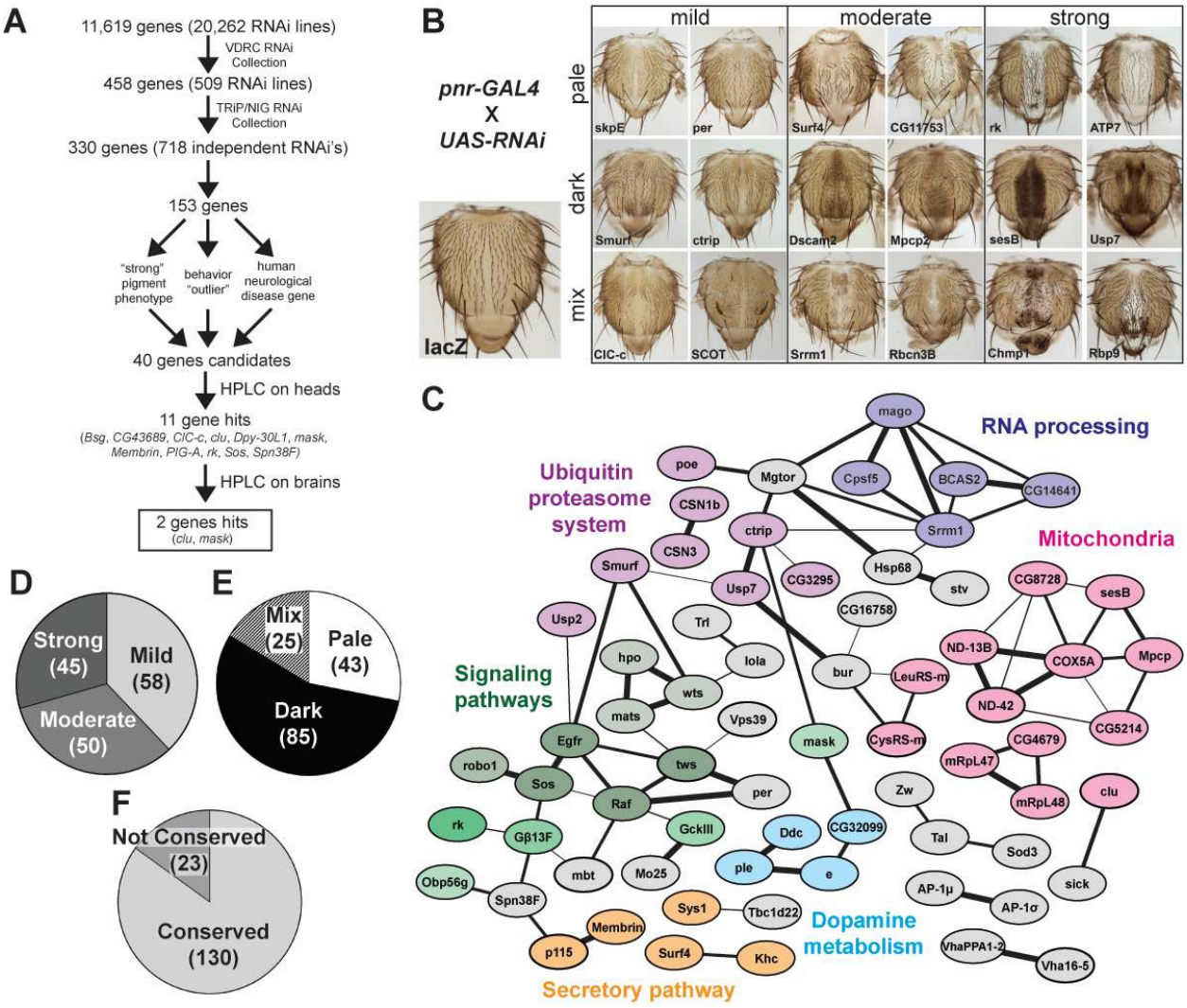

Fig 2. RNAi pigmentation screen reveals a broad spectrum of phenotypes and classes of genes (A) Flow chart depicting screening process. (B) Examples of the phenotypes observed from the RNAi-based pigmentation screen. (C) Protein-protein interaction network for 153 high confidence pigmentation gene hits from the RNAi-screen using STRING network analysis. Strength of line indicates confidence or strength of data support. Genes with no known interactions are not displayed. (D-F) Pie charts for the 153 pigmentation gene hits, including strength of phenotype (D), phenotype color (E), and conservation (F).

149 Our RNAi-based secondary screen produced a spectrum of phenotypes (Fig 2B), but the
150 phenotypes strengths (mild, moderate, or strong) were equally represented (mild = 38%,
151 moderate = 33%, strong = 29%, Fig 2D). Pigmentation color changes were classified in three
152 primary categories, pale, dark, or mix (a combination of pale and dark in a single thorax), which
153 were not equally represented (Fig 2E). Dark cuticle phenotypes were the most common (56%),
154 with pale and mixed cuticle phenotypes seen in 28% and 16% of genes, respectively.

155 We performed a protein-network analysis (Fig 2C) and found a group of proteins
156 previously linked to cuticle pigmentation as well as clusters related to RNA processing, ubiquitin
157 proteasome system, mitochondria-associated proteins, and signaling pathway genes, Hippo and
158 EGF (epidermal growth factor) signaling in particular. GO enrichment analysis highlighted terms
159 associated with cuticle pigmentation, protein stability, and several signaling pathways (S1 Fig).
160 We also observed that 85% of our genes were conserved between *Drosophila* and human, an
161 enrichment from the 68% of conserved genes in the original screen (Fig 2F and S2 Fig).

162 In summary, the cuticle pigmentation screen identified a spectrum of pale, dark and mixed
163 phenotypes in 153 genes, showing a validation of ~50% from the original screen. Close
164 examination of these hits highlights conserved molecular processes.

165 Many pigmentation genes isolated have a neurological
166 consequence

167 To investigate if our gene candidates have a neurological consequence, we first
168 checked if their homologs are associated with a neurological disease. We found that 51.2% of the
169 fly gene homologs are associated with a disease, 78% of those have at least one disease with
170 neurological phenotypes (Table 1 and S2 Fig), such as intellectual disability, autism spectrum
171 disorder, ataxia, epilepsy, and cerebral atrophy.

172 **Table 1. Fly pigmentation genes identified from this screen with neurological disease**

173 **associated homologs in human.**

Fly Gene	Human Homologs with Neurological Phenotypes (DIOPT Score, Max=18)	Notable Neurological Phenotypes
AP-1sigma	AP1S2 (12), AP1S1 (11), AP2S1 (3)	ataxia, DD, seizures
ATP7	ATP7A (13), ATP7B (13)	dystonia, neurodegeneration, seizures, tremor
Atu	LEO1 (10)	ASD
byn	TBXT (11), TBX19 (10)	neural tube defects, seizures
CG16758	PNP (14)	ataxia, behavioral problems, spastic diplegia, tremor
CG4328	LMX1B (10)	spina bifida
CG43689	MYT1L (7)	DD, ID
CG4679	PTCD3 (14)	cerebral atrophy, myoclonus, psychomotor delay
CG5902	AAMERCR1 (13)	cerebral atrophy, early motor delay, myoclonus
CG8728	PMPCA (15)	ataxia
ClC-c	CLCN3 (12), CLCN4 (11), CLCNKA (3)	ID, language delay, seizures, structural abnormalities
ctrip	TRIP12 (10)	delayed speech, ID, psychomotor delay
Cyp301a1	CYP24A1 (5), CYP27B1 (4), CYP27A1 (4)	ataxia, motor delay, psychiatric symptoms, seizures
CysRS-m	CARS2 (15)	cerebral atrophy, epilepsy, psychomotor delay
Ddc	DDC (14), HDC (4)	dystonia, psychomotor delay, sleep disturbance
Dgp-1	GTPBP2 (3)	ataxia, dystonia, ID, psychomotor delay, seizures
Dscam2	DSCAM (10)	ASD
Egfr	ERBB4 (10), ERBB2 (10), ERBB3 (9)	ALS, axonal neuropathy, DD, seizures
Gbeta13F	GNB1 (15), GNB4 (13), GNB2 (12), GNB5 (3)	ADHD, CMT, DD, ID, language delay

gig	TSC2 (13)	brain structural abnormalities, seizures
Hrb98DE	HNRNPA2B1 (12), HNRNPA1 (9)	ALS, dementia, motor neuropathy
Itpr	ITPR1 (14), ITPR3 (11)	ataxia, cerebellar atrophy, motor delay
Khc	KIF5C (12), KIF5A (12)	ALS, psychomotor delay, seizures, spastic paraplegia
Larp7	LARP7 (10)	anxiety, DD, ID, unstable gait
LeuRS-m	LARS2 (15)	cognitive impairment, DD, dystonia, tremor, seizures
mask	ANKRD17 (10)	DD, ID, motor delay, speech delay
mbt	PAK1 (3), PAK3 (3), PAK2 (3)	ID, macrocephaly, seizures, speech delay
Membrin	GOSR2 (13)	cerebral atrophy, DD, seizures
Mp	COL18A1 (6)	ataxia, seizures
Mpcp2	SLC25A3 (14)	motor delay
ND-13B	NDUFA5 (13)	ASD
ND-42	NDUFA10 (14)	DD, strutural abnormalities
Npc2b	NPC2 (7)	behavioral problems, DD, dementia, dystonia, seizures
per	PER3 (8), PER2 (7)	sleep abnormalities
PIG-A	PIGA (15)	seizures, structural abnormalities
ple	TH (15)	ataxia, dystonia, Parkinsonism, motor and sleep delay
Prosap	SHANK2 (10), SHANK3 (8)	ASD, DD, schizophrenia, seizures
Raf	BRAF (14), RAF1 (11)	DD, seizures
Rbp9	ELAVL2 (12), ELAVL3 (10)	ASD
rdx	SPOP (10)	DD, ID, speech delay
robo1	ROBO3 (8)	structural abnormalities

SCOT	OXCT1 (15)	coma, psychomotor delay
sesB	SLC25A4 (12)	motor delay, hyperreflexia
slp1	FOXG1 (6), FOXI1 (3), FOXJ1 (3), FOXC1 (3)	dystonia, motor delay, sleep and structural abnormalities
Smurf	ITCH (4), NEDD4L (3)	ID, psychomotor delay, seizures
Sod3	SOD1 (4)	ALS, spastic tetraplegia
Sos	SOS1 (14), SOS2 (12)	cognitive impair, learning disabilities
Spn38F	SERPINC1 (4), SERPINI1 (4)	cerebral atrophy, dementia, seizures
stv	BAG3 (9)	abnormal gait, behavioral problems, neuropathy
tws	PPP2R2A (13)	ataxia
Usp2	USP8 (4)	behavioral problems
Usp7	USP7 (13)	ID, psychomotor delay, seizures, structural abnormalities

174

175 **Table 1.** Homologs were defined as a Drosophila Integrative Orthology Prediction Tool (DIOPT,
176 version 8.0) score greater than or equal to three. Neurological disease associations were based
177 on Online Mendelian Inheritance in Man (OMIM)_clincal disease phenotypes and high-confident
178 ASD genes listed in Simons Foundation Autism Research Initiative (SFARI) gene database (class
179 S, 1, 2 or 3). ASD=Autism Spectrum Disorder, DD=Developmental Delay, ID=Intellectual
180 Disability, ALS=Amytrophic Lateral Sclerosis, CMT=Charcot-Marie-Tooth disease.

181

182

183 Since dopamine is known to regulate locomotion and sleep (22,33), we screened for
184 locomotion and sleep defects using the Drosophila Activity Monitor (DAM) (34). We tested 274
185 RNAi lines from the NIG, TRiP, and VDRC RNAi collections (35–37) corresponding to the
186 validated 152 gene hits. We scored the lines for total locomotion, total sleep, sleep bout length,
187 and sleep latency during the night and day (Fig 3). There was a broad range in the RNAi lines for
188 each of these phenotypes (Figs 3C). We classified RNAi lines “outliers” if they were two standard
189 deviations from the mean for a given phenotype (locomotion: 23 lines, total sleep: 20 lines, sleep
190 bout length: 21 lines, sleep latency: 25 lines). While total sleep and locomotion strongly
191 overlapped with each other, sleep latency and sleep bout length did not overlap with the other
192 sleep phenotypes (Fig 3D). We assessed if certain gene categories (>10 genes) showed any
193 distinct behavioral patterns (Fig 2C). There was no change in total locomotion or total sleep in the
194 categories assessed (Fig 3F and 3G). However, each categories showed a distinct pattern in
195 sleep bout length and latency (Fig 3F and 3H). This could indicate a distinction in how different
196 gene functions could affect sleep. Since genes that affect sleep can often show distinct
197 phenotypes that do not necessarily correspond to multiple phenotypes or times of day (38), any
198 gene with one phenotype during the day or night was classified as an “outlier”. This produced
199 sixty lines, corresponding to 50 genes.

200

201 **Figure 3**

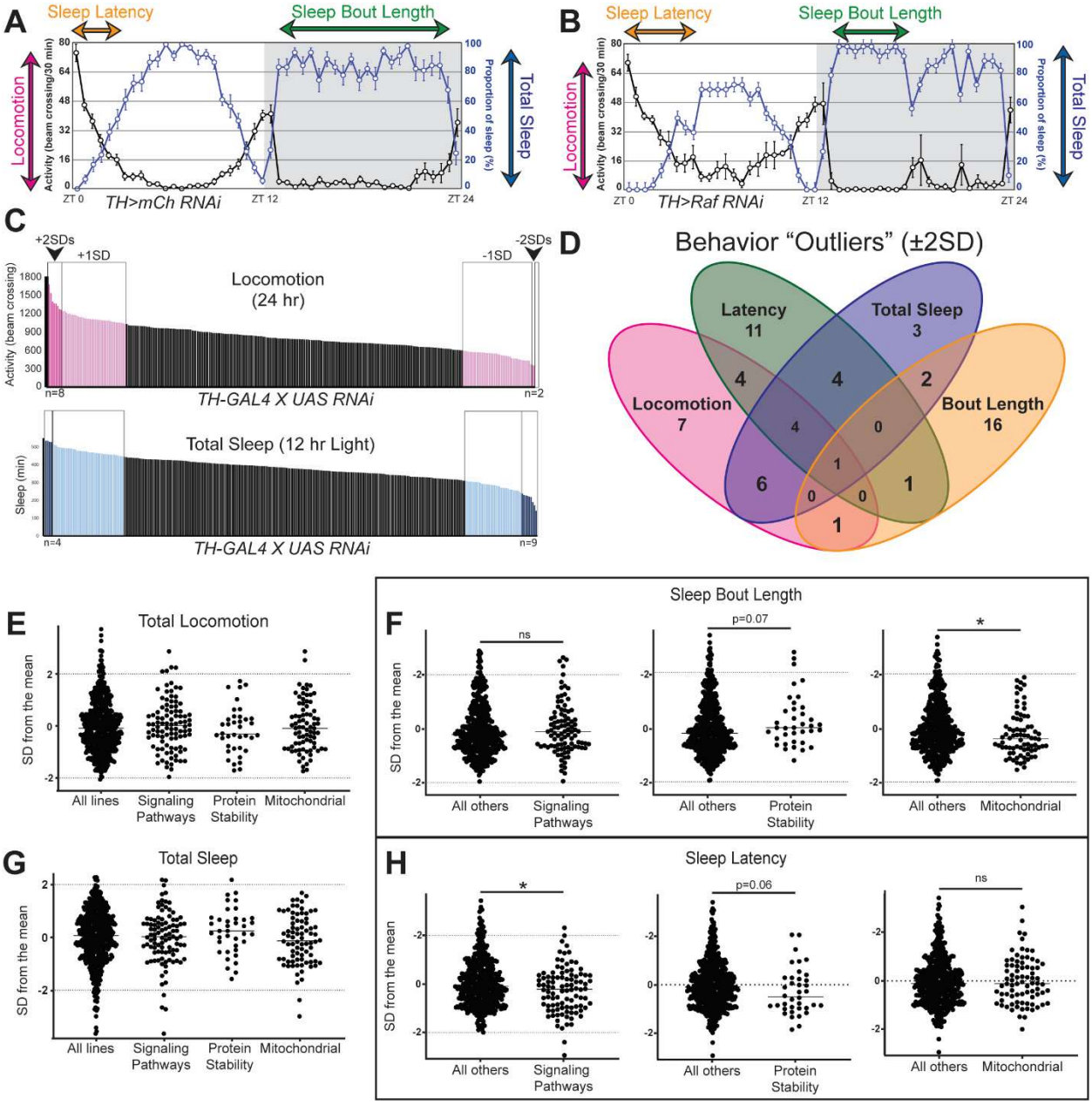

202
203

204 **Fig 3. *Drosophila* Activity Monitor (DAM) screen identifies behavior "outliers" and**
205 **highlights distinct phenotypes for gene categories.** (A-B) Representative activity and sleep
206 data measured in a neutral RNAi line (*mCherry RNAi*, A) and a behavioral "outlier" (*Raf RNAi*,
207 B) knocked down in DANs (*TH-GAL4*). (C) Bar graph showing all RNAi lines tested for 24hr
208 locomotion and total sleep during the 12hr light period, where light pink/blue represents fly lines
209 ±1SD away from the mean, and dark pink/blue are fly lines ±2SDs away from the mean (a.k.a.
210 "outliers"). (D) Venn diagram of "outliers" for the four phenotypes examined (sleep latency, sleep
211 bout length, locomotion, and total sleep). (E-H) Behavioral analysis of lines in three gene
212 categories captured in the pigmentation screen, including locomotion (E), sleep latency (F),
213 sleep bout duration (G), and total sleep (H). Individual t-tests were performed to assess if genes
214 in a category were significantly different to all other genes tested, and only those with a $p<0.10$
215 are reported, with *=$p<0.05$.

216

217

218 Taken together, 77 of our 132 conserved genes are likely to have a neurological function,
219 because they are implicated human neurological disease (52 conserved genes) or were classified
220 as a behavioral “outliers” (45 conserved genes).

221 11 genes alter dopamine levels in the fly head

222 To prioritize our gene list for dopamine measurement, we identified conserved genes (132
223 conserved/152 pigmentation genes). Then, we prioritized these based on whether knockdown of
224 these genes showed a strong pigmentation effect (38 genes), a behavioral effect in the DAM (45
225 genes), and/or a human neurological disease association (52 genes). 72% (95/132 conserved
226 genes) were represented in one of these categories, and 29% (39/132) were represented in at
227 least two (Fig 4A). We classified genes in two or more categories as priority hits and tested them
228 for changes in dopamine using High Performance Liquid Chromatography (HPLC). We repeated
229 previous results showing that knocking down *TH* or overexpressing a *TH* cDNA using *TH-GAL4*
230 significantly reduces or increases head dopamine without effecting serotonin (Figs 4B and 4C)
231 (29).

232

Figure 4

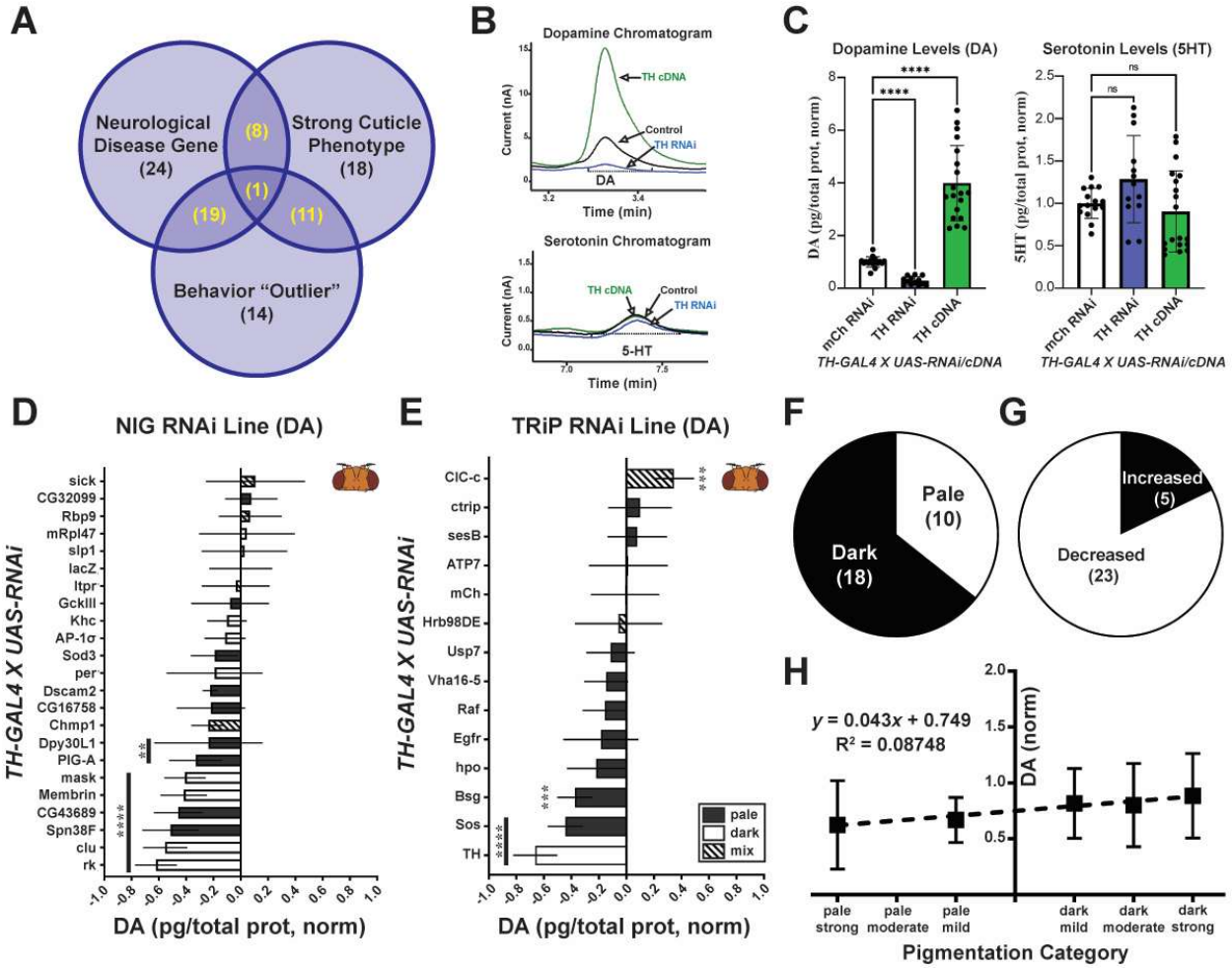

Fig 4. Eleven genes alter head dopamine upon knockdown. (A) Venn diagram of the categories used to prioritize 39 genes (in yellow). (B) Representative chromatograms for dopamine (DA) and serotonin (5-HT) upon knockdown or overexpression of TH in Dopaminergic cells (*TH-GAL4*). (C) Quantification of DA and 5-HT from chromatograms. (D-E) HPLC analysis on prioritized genes for UAS-RNAi lines from NIG (D) and TRiP (E). Pie charts for all genes for cuticle color (F) and trend in dopamine (G). (H) XY plot comparing pigmentation phenotype to dopamine levels. For (C) Brown-Forsythe ANOVA test performed with Dunnett's T3 multiple comparisons test. For (D) and (E) ordinary One-way ANOVA test with Dunnett's multiple comparisons test. **=p<0.01, ***=p<0.001, ****=p<0.0001. Error bars represent SD.

245 We found that 11 of 35 prioritized genes (note: some not tested due to lethality or stock
246 issues) significantly altered head dopamine levels (Figs 4D and 4E). Since control NIG lines
247 showed about ~80% dopamine levels compared to the TRiP collection (S3 Fig), we compared
248 the DA levels to control lines appropriate for each collection (e.g. UAS-lacZ RNAi). Unlike cuticle
249 pigmentation, where 65% of genes caused a dark cuticle (excludes mixed cuticle phenotype),
250 most genes trended toward a reduction in dopamine (71%, 25/35, Figs 4F and 4G). There was
251 no correlation between the cuticle color and the dopamine level in the fly head (Fig 4H).

252 In summary, our HPLC analysis on fly heads revealed 11 genes that significantly affect
253 dopamine levels. We saw a trend in reduction in dopamine across all lines tested, and we
254 observed no correlation between cuticle color and dopamine level.

255 Brain study reveals *mask* and *clueless* as potential regulators
256 of brain dopamine

257 To determine which of the 11 genes that affect dopamine in the head have consequences
258 on the brain, we examined the expression of four of them in the brain using available T2A-GAL4
259 lines (39–41). We found that several overlapped with somewhere between 25% - 100% of DANs
260 (S5 Fig, Figs 5B and 5G). In publicly available single-cell mRNA sequencing datasets, ten of our
261 gene hits (all except *Spn38F*) show expression in the brain with varying overlap with TH
262 expressing DANs (42,43).

263

Figure 5

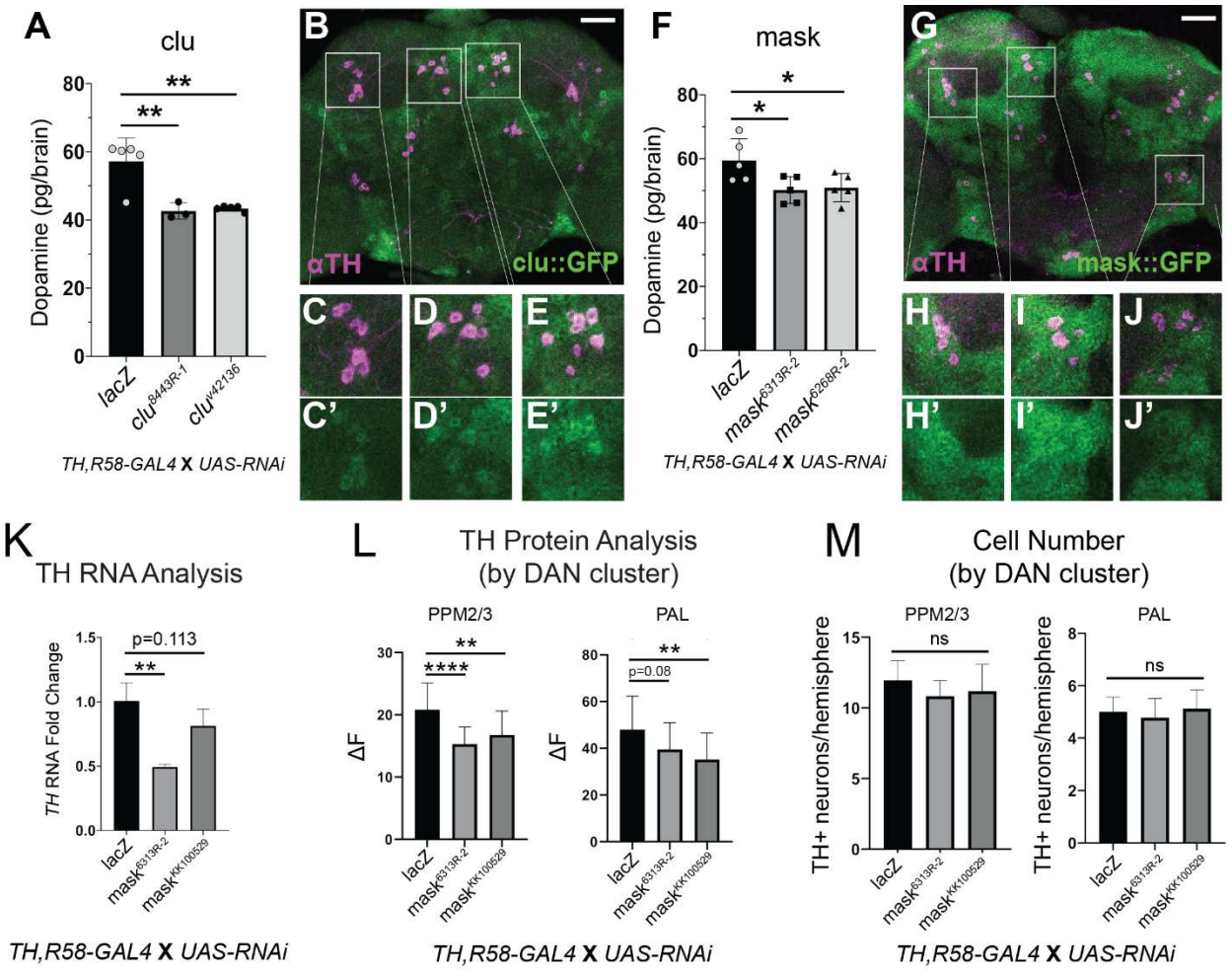

Fig 5. Brain dopamine analysis identifies *mask* and *clu* as novel regulators of dopamine levels in the fly brain (A) Total dopamine in the adult fly brain upon knockdown of *clu*. (B) *clu::GFP* expression pattern in the adult brain (B-E, B'-E'). (F) Total dopamine in the adult fly brain upon knockdown of *mask*. (G) *mask::GFP* expression pattern in the adult brain (H-J, H'-J'). (K) qRT-PCR of TH upon *mask* knockdown with the recombined DAN (*TH, R58-GAL4*) driver. (L) Quantification of total TH protein level through immunofluorescence in DAN clusters upon knockdown of *mask*. (M) Quantification of TH positive (TH+) neurons in DAN clusters upon knockdown of *mask*. Ordinary one-way ANOVA was done with Dunnett's multiple comparisons test (F, I, N). Error bars represent SD. Scale bars are 50 μm.

275 The *TH-GAL4* line commonly used for dopamine studies misses a large portion of DANs,
276 particularly in the PAM cluster (~87 DANs missed/~142 total DANs per hemisphere) (44), making
277 it not ideal for quantifying total changes in brain dopamine. We recombined the *TH-GAL4* with
278 another driver that hits a large portion of the PAM cluster neurons (*GMR58E02-GAL4 or R58-*
279 *GAL4)* (18) generating a recombined line (labelled *TH,R58-GAL4*) that hits ~95% of DANs (S4
280 Fig).

281 We microdissected adult fly brains and measured dopamine for our 11 gene hits. Most of
282 them showed no change in brain dopamine (S5 Fig), but *mask* (*multiple ankyrin repeats single*
283 *KH domain*) and *clueless* (*clueless*) knockdown reduced total brain dopamine for two independent
284 RNAi lines (Figs 5A and 5F). Protein trap lines (45,46) for both Clueless and Mask show broad
285 expression patterns in the brain (Figs 5B-5EJ-5M and 5G-5J). When we focused on DAN clusters
286 (e.g. PPL1 and PPM2), Clueless protein appears to be enriched in DANs (Figs 5C-5E and 5C'-
287 5E'), whereas Mask shows a broad and equal expression throughout most cells in the brain (Figs
288 5H-5J and 5H'-5J').

289 In summary, our fly brain analysis revealed two genes that (18%, 2/11) significantly altered
290 brain dopamine.

291 *mask* regulates Tyrosine Hydroxylase and alters sleep in a 292 dopamine-dependent manner.

293 To test if *clu* and *mask* knockdown could be due to DAN loss, we quantified the number
294 of DANs in several clusters (44). There was no difference in neuron number for every cluster
295 examined (Fig 5M and S6 Fig). Since our pigmentation gene study revealed that only the
296 manipulation in TH reduced brain dopamine (Fig 1), we examined if knocking down *clu* or *mask*
297 affects *TH* RNA or protein level. Knockdown of *mask* led to a significant reduction in *TH* mRNA

298 level for one RNAi (50% reduction), with the other RNAi trending (20-30% reduction, Fig 5K).
299 Upon examining TH levels in different DAN clusters, two clusters showed significant reduction in
300 TH protein level, with other clusters showing a trend in TH protein reduction (PAL and PPM2/3,
301 Fig 5L and S6 Fig). To assess behavioral consequences, we performed additional sleep analysis
302 on *mask*. Dopamine is a wake-promoting agent, and complete loss of dopamine in the brain
303 significantly increases sleep (47,48). Knocking down *TH* using the *TH-GAL4* did not significantly
304 alter total levels of sleep during light or dark periods (S7 Fig), which may be due to the selective
305 expression of the GAL4 or the partial reduction of dopamine (Fig 4C). However, there was a
306 significant increase in sleep in the two hours before light onset, which is classified as light
307 anticipation. Similarly, knockdown of *mask* with the TH-GAL4 showed a highly consistent
308 reduction in light anticipation (Fig 6A, 6B, 6B', and S8 Fig). When we feed the flies L-DOPA, the
309 effect is no longer seen (Fig 6C, S8 Fig). Additionally, in *Drosophila* caffeine's effects on sleep
310 are mediated by dopamine through a point that is upstream of L-DOPA, potentially via TH activity
311 (49). Based on this, we suspected that *mask* knockdown would ameliorate the effects of caffeine
312 on sleep, since *mask* appears to reduce the synthesis of *TH*. We saw that caffeine's effect on
313 total sleep and sleep in the dark is ameliorated upon *mask* knockdown (Fig 6D, 6E, and S8 Fig).

314

315 **Figure 6**

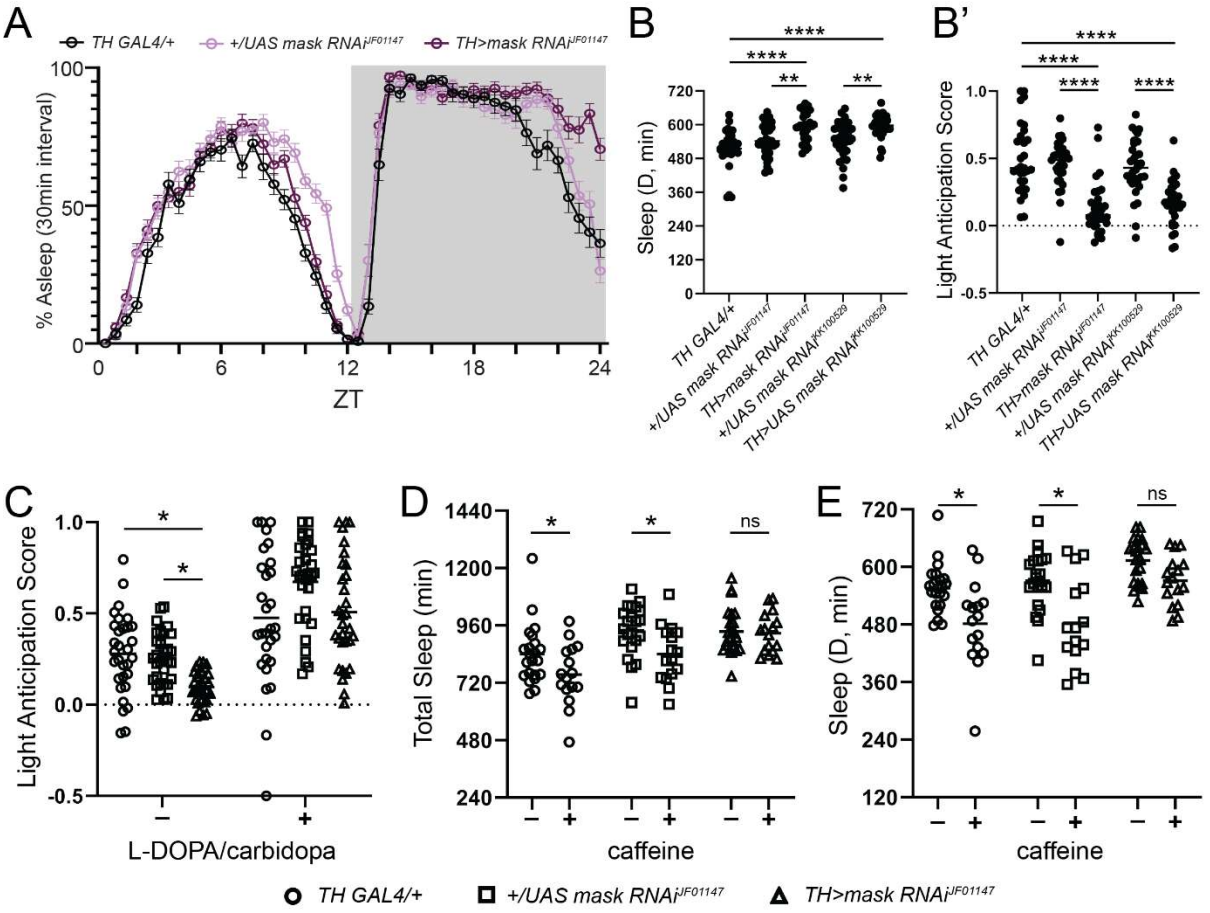

316

317 **Fig 6. *mask* knockdown reduces TH mRNA and protein and causes sleep phenotypes**
318 **that align with reduction in TH levels** (A) 24-hr sleep graph (sleep binned in 30-minute
319 intervals) upon mask knockdown using the TH-GAL4. (B) Quantification of total sleep
320 throughout the 12-hr dark period upon mask knockdown (B') Quantification of light anticipation
321 upon mask knockdown. (C) Light anticipation in mask knockdown flies with L-DOPA feeding. (D-
322 E) Caffeine effects on sleep upon mask knockdown – (D) Total Sleep and (E) Sleep during the
323 12-hr dark period. For samples with more than one experimental, ordinary one-way ANOVAs
324 were performed with Dunnett's multiple comparisons. (B, B', C). For samples with one
325 experimental, individual t-tests were performed (D,E). *=p<0.05, **p<0.01, ****p<0.0001. Error
326 bars represent SD.

327 Follow up studies on *clueless* showed that *clueless* knockdown increases TH RNA level
328 by about 1.5-2X, with no effect on TH protein level or TH+ neurons (S9 Fig), and while there
329 was an increase in sleep across several RNAi lines, there is no light anticipation phenotype.
330 Feeding TH>clu RNAi flies L-DOPA was unable to rescue the *clueless* effects on sleep (S9 Fig),
331 suggesting that the effects on dopamine and TH may be a secondary effect. Additionally, the
332 antioxidant NACA was also unable to rescue the sleep defects seen upon *clueless* knockdown.

333 In conclusion, *mask* appears to reduce total dopamine levels and sleep by affecting
334 transcription of TH, while *clueless* is acting through an alternative mechanism.

335 Discussion

336 Validation of 148 novel cuticle pigmentation genes

337 Our RNAi screened confirmed 153 genes that were previously implicated in *Drosophila*
338 pigmentation – 148 of these genes have not been previously associated with dopamine biology.
339 Because we observed a strong enrichment for genes involved in pigmentation and tyrosine
340 metabolism (S1 Fig), our method for screening and analysis effectively identified genes that play
341 critical roles in the biological process of interest.

342 While prior research has compared genes that overlap with different types of screening
343 strategies (e.g. chemical mutagenesis vs. RNAi), most RNAi phenotypes from large-scale screens
344 have not been validated with alternative RNAi lines or collections. The original source RNAi
345 screen used the lines available at the VDRC stock center (35,37). Alternative sources for RNAi
346 lines (i.e. TRiP and NIG) start with different backgrounds, vectors, hairpin lengths, insertion
347 methods, and/or target different areas of the gene (36,50). This allow researchers to overcome
348 the off-targeting and weak silencing seen with RNAi analysis, but to our knowledge, there have

349 been no screens or meta-analyses to systematically test consistency across lines from different
350 sources. In this study, we found that ~46% (153/330) of genes with a pigmentation phenotype
351 showed a phenotype in an alternative RNAi, and 87% of those phenotypes showed agreement in
352 pigmentation color, highlighting that pigmentation as a phenotype is relatively consistent (S10
353 Fig).

354 Interestingly, 85% of our pigmentation genes had at least one homolog, whereas genes
355 tested in the original RNAi screen list only had ~68% conservation (1.25-fold enrichment, S2 Fig).
356 Even though pigmentation of the cuticle through dopamine and its synthesis enzymes, produced
357 through TH and Ddc, is an invertebrate-specific phenomenon (12), the enrichment for conserved
358 genes suggests that this phenotype is relevant for some conserved biological pathway and
359 mammalian biology. We propose that cuticle pigmentation in insects may be a "phenolog" (51) of
360 certain neurological traits in mammals

361 Protein-protein interaction network highlights unexpected 362 gene associations

363 When we investigated what kind of gene categories were found in the pigmentation
364 screen, we saw clusters of genes that are associated with ubiquitin-proteasome system (UPS),
365 RNA processing, mitochondria, and developmental signaling pathways. Each of these processes
366 could be relevant to dopamine biology. For example, there is some evidence that the UPS system
367 regulates TH levels in the mammals since inhibition of the UPS system has been shown to
368 increase the TH protein in a PC12 rat cell line (52,53). In addition, changes in RNA processing
369 could indicate changes in the dopamine synthesis enzymes TH and Ddc since these enzymes
370 undergo RNA processing to create two different isoforms (54). The two TH isoforms differ in tissue

371 expression and kinetics(55). In mammals, post-transcriptional trafficking of TH mRNA and
372 translational regulation has been suggested to be important for its function (56).

373 We identified 12 genes that are known to function at the mitochondria, mostly in the
374 electron transport chain (*ND-13B*, *ND-42*, *COX5A*), mitochondrial mRNA translation (*mRpL47*,
375 *mRpL48*, *CG4679*), and mitochondrial protein localization (*CG8728*, *clu*, *mask*, *Mpcp2*). It is well-
376 known that the mitochondria have a key role in dopamine metabolism in mammals since MAO
377 acts in the mitochondria to degrade dopamine. However, there is no known MOA homolog in
378 flies(12). Interestingly, the metabolites for oxidation and methylation of dopamine (DOPAC and
379 HVA) have been observed in flies (57–60). In addition, mutants for enzymes thought to be the
380 primary regulators of dopamine degradation (*ebony*, *tan*, and *speck*) (61,62) did not have any
381 effect on dopamine in the brain (Fig 1), suggesting an alternative process regulates dopamine
382 degradation in the brain. It is plausible that mitochondria could be involved in this process.

383 The last major group of genes identified from our screen was developmental signaling,
384 specifically EGF signaling and Hippo signaling. To date, neither EGF nor Hippo signaling have an
385 established connection with dopamine biology in *Drosophila*. We may have pulled these genes
386 out is because the process of forming the dorso-central thorax is developmentally regulated (63–
387 65). However, we did not identify core components of the other key pathways, such as Notch or
388 Hedgehog, suggesting that EGF and Hippo are more specifically involved in this pigmentation
389 process.

390 Cuticle pigmentation phenotypes may not reflect changes in 391 dopamine

392 The field has generally assumed that a darker cuticle reflects an elevated level of
393 dopamine (15,66). However, when we measured dopamine from degradation enzyme mutants

394 using HPLC, we saw either no effect on dopamine level or reduced level of dopamine in the head.
395 In addition, when we measured dopamine from the pigmentation genes from the screen, a darker
396 cuticle did not reflect elevated levels of dopamine in the head. While we were able to increase
397 dopamine by 3-5 fold upon TH cDNA overexpression in the head (Fig 4C), this phenomenon was
398 not observable in the brain. One reason could be that there is a selective pressure or a strong
399 feedback mechanism that prevents elevated levels of dopamine in the nervous system. Since
400 oxidized dopamine could be toxic (67), this could be a mechanism to prevent cell toxicity.
401 Regardless, changes in cuticle pigmentation do not necessarily reflect changes in dopamine level,
402 so assumptions should not be made that increase in melanin levels in the fly corresponds to
403 increased levels of dopamine.

404 Upon seeing alterations of dopamine in the head for some of the classic pigmentation
405 genes, we next wanted to test if this corresponded to changes in the brain. In the case of
406 established dopamine metabolism genes, we only saw a change in dopamine levels upon
407 reduction of TH. When we looked at expression for some of these genes, we saw that all the
408 genes we were able to assess (*black*, *speck*, *tan*) were expressed in the brain, but their expression
409 did not overlap well with DANs. It may be that dopamine degradation does not happen in the
410 neurons since it was hypothesized to occur in the glia (31,68). However, the expression does not
411 seem to show a broad glial expression using the reagents we had access to. For the 11 genes
412 from the pigmentation RNAi screen that showed altered levels of dopamine, only 2 (18%) of them
413 showed an effect on dopamine in the brain. Hence, head dopamine levels should not be used as
414 a proxy for brain dopamine levels.

415 *clu* and *mask* reduces brain dopamine levels through different 416 mechanisms

417 Once we identified that knockdown of *clueless* and *mask* both reduced dopamine in the
418 brain without affecting the number of DANs, we hypothesized that they may be acting through TH
419 since our initial dopamine metabolism studies showed that only changes in TH significantly
420 affected dopamine levels in the brain.

421 *mask* encodes a scaffolding molecule that functions in multiple contexts (69–71). In this
422 study, *mask* knockdown reduced both *TH* mRNA and protein levels, suggesting it acts on TH
423 transcription. Follow-up behavior analysis, showed that *mask* knockdown in DANs led to a highly
424 consistent change in sleep. Specifically, *mask* knockdown reduced the number of flies that
425 anticipated light. While fruit flies typically start to wake before light onset (72), loss of mask in
426 DANs suppresses this anticipation behavior. Supporting this mechanism, we saw a similar
427 phenotype with the TH RNAi and the DAN driver (TH>TH RNAi, S7 Fig). Dopamine is a wake-
428 promoting molecule, and if dopamine synthesis normally increases before light onset as a means
429 of waking the fly, reduced levels of TH could put strain on this mechanism.

430 When we fed *mask* knockdown flies the precursor for dopamine, L-DOPA, this abolished
431 the effect on light anticipation. We suspect that feeding L-DOPA does not override all sleep-
432 dependent effects because clueless sleep phenotypes remained when we fed them L-DOPA (S9
433 Fig). There is evidence that in the fruit fly caffeine affects sleep through TH. Specifically, Nall et
434 al. showed that caffeine's effect on sleep is absent in TH mutant flies, even if L-DOPA is given
435 (49). Since *mask* knockdown effects TH mRNA levels, we tested if mask knockdown would
436 suppress the effects of caffeine. We found that the reduction in total sleep and sleep during the
437 dark period normally seen upon caffeine administration were absent upon mask knockdown. This
438 further supports that mask alters TH levels.

439 While we do not have any direct evidence for how *mask* may be altering TH levels, *mask*
440 has been implicated in multiple biological pathways that were highlighted from our screen,

441 including EGF signaling (e.g. *Egfr*, *Sev*, Raf), Hippo signaling (e.g. *hpo*, *wts*, *mats*), and
442 mitochondrial biology (73–76). Egf and Hippo signaling have well-known transcriptional effects
443 (77,78), but whether they may regulate TH transcription directly or indirectly in this context need
444 further investigation. It is also possible that *mask* is acting in several of these pathways at once,
445 which causes it to have a strong additive effect that produces a significant change in dopamine
446 in the whole brain, while knockdown of individual pathway genes may have a more restricted role
447 (e.g. *Egfr*, *Sos*, *hpo*).

448 In addition to *mask*, we also saw that knockdown of *clueless* leads to significant reduction
449 in dopamine. However, when we explored the behavioral consequence of *clueless* knockdown, it
450 did not show the same effect on sleep as *mask* or *TH* knockdown. In addition, the sleep phenotype
451 was not rescued by L-DOPA, and molecular biology showed that *clueless* knockdown leads to an
452 increase in TH mRNA with no change in TH protein. Taken together, this indicates that the effect
453 on dopamine from *clueless* knockdown may be a secondary consequence. *clueless* encodes a
454 ribonucleoprotein thought to act at the outer mitochondrial membrane to promote proper formation
455 of protein complexes including mitophagy proteins like Pink1 and Parkin (79,80). It also interacts
456 with the ribosome and translocase complex at the mitochondrial membrane (79,81) suggesting it
457 acts as a regulator for mitochondrial protein translation and import. Knockdown of *clueless*
458 showed no effect on TH protein level, but since this is a mitochondrial protein, it may be more
459 likely that the effect on dopamine is through the previously proposed roles of mitochondria in
460 regulating dopamine levels.

461 In conclusion, while both genes cause a reduction in dopamine, *mask* appears to regulate
462 dopamine by altering TH levels, possibly through regulation of TH mRNA. On the other hand,
463 *clueless* effects on dopamine appear to be a secondary consequence, with a behavioral effect
464 that is independent of dopamine. Additional analysis on changes in enzymatic activity as well as
465 potential downstream targets would help identify how these genes are acting.

466 ## Some regulators of dopamine levels may act locally

467 When we examined the expression of some of our pigmentation genes in the brain (S11
468 Fig), we found that many of them do not overlap with all DANs. Indication that measuring global
469 changes in dopamine may not be best for determining effects on DA for many of these genes.
470 They may require targeted dopamine measurements, perhaps through a fixed or live reporter
471 (82,83). It is also possible to assess changes in dopamine using behavior, but this would require
472 detailed assessment for each gene since behaviors are often cluster specific (84).

473 In conclusion, our screen of identified novel pigmentation genes, a subset of which were
474 identified as novel regulators of dopamine *in vivo*. Unbiased forward genetic screens in model
475 organisms are powerful ways to identify unanticipated links between distinct biological pathways
476 and provide new molecular handles to study the functional connections between them. Application
477 of such strategies to the regulation of dopamine levels will likely continue to identify novel factors,
478 some of which will impact our understanding of human neurological and neurodevelopmental
479 diseases.

480 # Resource Availability

481 All data generated or analyzed during this study are included in this published article and its
482 supplementary information files. This study did not generate any new unique reagents.

483 # Acknowledgements

484 We thank the Bloomington *Drosophila* Stock Center (USA), the National Institutes Genetics Fly
485 Stock Center (Japan), *Vienna* Drosophila RNAi Center (Austria) and Dr. Hugo Bellen for providing
486 useful fly stocks and reagents for this project. We would like to thank Drs. Jonathan Andrews,

487 Hugo Bellen, Brigitte Dauwalder, Herman Dierick, Linsday Goodman, Oguz Kanca, Kartik
488 Venkatachalam, Michael Wangler, Sheng Zhang and Huda Zoghbi for useful suggestions,
489 discussions and advice on the overall project. This work was supported by startup funds to SY
490 from the Jan and Dan Duncan Neurological Research Institute at Texas Children's Hospital and
491 the Department of Molecular and Human Genetics at Baylor College of Medicine. Confocal
492 microscopy at BCM was supported in part by the Intellectual and Developmental Disabilities
493 Research Center (IDDRC, grant number U54HD083092) from the Eunice Kennedy Shriver
494 National Institute of Child Health & Human Development.

495 Authors Contributions

496 S.Y. and S.L.D. conceived the experiments and wrote the manuscript. S.Y., E.S.S., D.B., and
497 S.L.D. conducted the pigmentation screen and DAM behavior analysis screen. S.L.D. and K.W.
498 conducted the pigmentation mutant analysis experiments. S.L.D., S.B.G, H.D-S, Y.F., and K.W.
499 conduced the HPLC analysis. S.L.D. and Y.F. performed confocal imaging. S.L.D. conducted all
500 data analysis. All authors participated in the critical analysis of the manuscript.

501 Declarations of Interests

502 The authors declare no competing interests.

503 Materials and Methods

504 Fly Maintenance

505 Flies (*Drosophila melanogaster*) strains and crosses were reared at 25°C on a 12:12 Light/Dark
506 (LD) program unless stated otherwise. Flies were fed a molasses-based food source. Different
507 temperatures were used to achieve different levels of gene knockdown or overexpression, which

508 is documented for each experiment. Flies were transferred to a new vial 0-2 days post-eclosion
509 (dpe) for age-appropriate analysis. Experiments were run on 3-7 dpe flies unless otherwise stated.

510 Fly Stocks and Crosses

511 Mutant and transgenic trains were obtained from Bloomington *Drosophila* Stock Center (BDSC,
512 https://bdsc.indiana.edu/), Vienna Drosophila Research Center (VDRC,
513 https://www.viennabiocenter.org/vbcf/vienna-drosophila-resource-center/), the Japanese
514 National Institute of Genetics (https://shigen.nig.ac.jp/fly/nigfly/), or were gifts from scientists in
515 the field or generated in house (S1 Table – S5 Table).

516 For the cuticle screen *pnr-GAL4* (85) was crossed to the specified UAS-RNAi line (see S1 Table)
517 at 29°C, 25°C, and/or 18°C and examined after pigmentation is completed (>1 dpe). For the
518 behavior and HPLC analysis *TH-GAL4* females (also called *ple-GAL4*, BDSC stock #8848) were
519 crossed to the specified RNAi line (see S2 Table). For all HPLC analysis, the controls were
520 specific to the tested UAS-RNAi line (86). Thus, the TRiP collection of RNAi lines are compared
521 to the *UAS-mCherry(mCh) RNAi* line (BDSC #35785) and the NIG collection of RNAi lines as well
522 as the VDRC RNAi lines are compared to the *UAS-lacZ RNAi* line. For the HPLC analysis
523 performed on brains, we recombined the *TH-GAL4* with another DAN driver *GMR58E02-GAL4*
524 (BDSC #41347), which expresses in a large group DANs in the PAM cluster (27). These flies are
525 referred to as *TH,R58-GAL4* throughout the article. The *TH,R58-GAL4* line was also used for
526 qPCR and TH protein analysis via immunohistochemistry. For gene expression analysis *UAS-*
527 *mCh::nls* (BDSC #38424) females were collected and crossed with respective T2A-GAL4 lines
528 (see S5 Table). Female and males were both imaged at ~5-7dpe. For the follow up sleep studies,
529 the *UAS-RNAi* males were crossed with *TH-GAL4* virgins for the experimental. For the controls
530 w^{1118} females were crossed to males from either the *TH-GAL4* and *UAS-RNAi* lines
531 independently.

532 ## Notum Dissection and Imaging

533 For thorax analysis and dissection, males and females were both selected, though differences
534 were not generally observed, and females are shown here. Flies that were 3-5 dpe were collected
535 and placed in 70% EtOH. Notum dissection and imaging was previously published (87). In
536 summary, the thorax was dissected by removing the legs, abdomen, and head. Then the thorax
537 was cut such that a hole was on the ventral side to allow solution to pass into the thorax. These
538 dissected thoraces were placed in 10% KOH for 10 minutes at 90°C on a heat block. Then, the
539 KOH was removed and replaced with 70% EtOH solution. They were mounted on a slide prepared
540 with tape on two sides in mounting media (50% glycerol, 50% EtOH). The thoraces were imaged
541 on a stereo microscope (Leica MZ16) using OPTRONICS® MicroFIRE camera. The images are
542 z-stack brightfield images taken and collapsed using extended depth of field in Image-Pro Plus
543 7.0 and In-Focus (Version 1.6).

544 ## Brain Expression Analysis

545 Brain dissections and imaging were performed as previously reported (88). In summary, the
546 brains were dissected at 3-7 dpe in ice cold PBS and then fixed in 4% PFA in 0.5% PBST for 20
547 minutes. Then, they were washed with a quick wash in 0.5% PBST followed by three 10-20-
548 minute washes in 0.5% PBST while on a rotator. The samples were placed in primary antibody
549 solution [anti-Tyrosine Hydroxylase 1:500, PelFreez Biologicals, rabbit, P40101; anti-elav 1:100,
550 Developmental Studies Hybridoma Bank, rat, 7E8A10 in solution (5% Normal Donkey Serum,
551 0.1% NaN_3 in 0.5% PBST)] at 4°C for 3 days. Then, the samples were washed with a quick wash
552 in 0.5% PBST followed by three 10-20-minute washes in 0.5% PBST while on a rotator. After the
553 last wash, the samples were placed in a secondary antibody solution [anti-Rabbit 1:200 (Thermo
554 Fisher Sci., Alexa-647, A-21208); anti-rat 1:200 (Thermo Fisher Sci., Alexa-488, A-27040) in

555 solution (5% Normal Donkey Serum, 0.1% NaN_3 in 0.5% PBST)] for two hours at room
556 temperature. The samples were washed again with one quick wash followed by three 10-20
557 minutes washes in 0.5% PBST on a rotator. Then, the brains were mounted in Vectashield
558 mounting media and imaged on a confocal microscope (Zeiss LSM 710 or Zeiss LSM 880). All
559 images shown in this manuscript are Z-projection images that were generated using the ZEN
560 software (Zeiss).

561 RNAi-based Pigmentation Screen

562 We identified pigmentation gene hits from a primary screen performed in Jurgen Knoblich's lab
563 using the Vienna Drosophila Resource Center collection of RNAi lines by accessing their public
564 RNAi screen database (https://bristlescreen.imba.oeaw.ac.at/start.php). The original screen was
565 performed on 20,262 RNAi lines, encompassing 11,619 genes (~82% of protein-coding genes)
566 (22). We selected genes that showed a cuticle pigmentation score for any RNAi line tested (gene
567 scores ranged from two to ten). To validate pigmentation defects, we selected genes that had
568 RNAi lines within the Fly National Institute of Genetics (NIG, 220 genes, 426 RNAi lines) or the
569 Harvard Transgenic RNAi Project (TRiP, 221 genes, 292 RNAi lines) collections. Each RNAi line
570 was tested at 29°C and 25°C. If there was no phenotype no further testing was performed. If it
571 was lethal, we tested it at 18°C.

572 Classification of Cuticle Phenotypes

573 Phenotypes were scored using a qualitative scoring system. This system used *UAS-TH RNAi* and
574 *UAS-ebony RNAi*, some of the strongest regulators of cuticle color, as a baseline for the "strong".
575 Then, the other lines were placed along the spectrum as mild, moderate, or strong. Phenotypes
576 were scored by two independent observers and differences were settled by a third independent
577 observer. If there was variability with one line or if there was variability amongst lines, this might

appear as mild-moderate, moderate-strong, or mild-strong. In these cases, the strongest phenotype observed was documented as the recorded phenotype for a given gene.

Protein-protein interaction network and gene ontology analysis

The protein-protein interaction network was generated using STRING (search tool for recurring instances of neighboring genes; https://string-db.org/). This database includes protein-protein interactions that are physical interactions and functional associations. For our data set we included these sources of interactions: gene neighborhoods (genes that are found close together across species) (89), curated databases (publicly available databases of protein interactions), and experimental evidence (known complexes and pathways from curated sources) (90,91). Any genes that did not interact with other genes from our screen were not included in the interaction network. This database was last accessed on 05/05/2023. The lines between genes represents the confidence in the interactions, which is based on complex algorithms that are dependent on the source.

The gene ontology analysis was generated using GOrilla (Gene Ontology enRIchment anaLysis and visuaLizAtion tool, https://cbl-gorilla.cs.technion.ac.il/). The 153 pigmentation genes hits were included as target genes, and the background genes were the entire VDRC RNAi collection included in the Mummery-Widmer et al. 2009 screen. Only the GO terms with a p-value greater than 0.001 and a fold enrichment of greater than three were included in the analysis. Redundant terms were removed using Revigo (http://revigo.irb.hr/) with a stringency of 0.7. Those that have a fold enrichment greater than five were included in S1 Figure.

Human Neurological Disease Gene Classification

600 Homologs for each fly gene were identified using DIOPT (DRSC Integrative Ortholog Prediction
601 Tool, v8.0, https://www.flyrnai.org/diopt) (92). Genes were classified as orthologs if they had a
602 DIOPT score≥3. The human genes were scored as neurological disease-causing genes if they
603 had an OMIM (Online Mendelian Inheritance of Man, last accessed 01/01/2023,
604 https://www.omim.org/) disease association with any documented neurological phenotype (93).
605 Genes were also classified as human neurological disease genes if they were in the Simons
606 Simplex Collection of Autism Spectrum Disorder gene list (last accessed 06/01/2022,
607 https://gene.sfari.org/) and had a score equal to or less than 3 (1, 2, or 3) and/or syndromic (S)
608 (94).

609 Behavior Analysis using the *Drosophila* Activity Monitor

610 Behavior screen

611 For the behavior screen, the crosses were set in a 12:12 LD chamber at 25°C and transferred
612 every 2-3 days to increase the number of progenies. Upon eclosion, flies were transferred to 29°C
613 and kept for 2-3 more days before testing. Individual tubes (PPT5x65 Polycarbonate, Trikinetics
614 Inc, USA) appropriate for use with the *Drosophila* Activity Monitor (DAM, Model DAM2 for 5mm
615 tubes, TriKinetics Inc, USA) were loaded with approximately ½" worth of molasses-based food.
616 The end of the tube with food was sealed by placing the vial into Paraplast® (Sigma-Aldrich) wax
617 three times and allowing it to dry. Once they were dry, individual male flies were placed into each
618 vial, the vial was placed into the DAM recording chamber, and it was sealed using a 5mm tube
619 cap (CAP5, TriKinetics Inc, USA) with a hole stuffed with cotton. For each genotype, 16 individual
620 males were run, except in a few cases where we were unable to get that many flies. In which
621 case, as many living males as possible were run. The flies were loaded into a 12:12 LD chamber
622 at 29°C and monitored for 3 days. Then, the flies were removed and dead flies were eliminated
623 from analysis.

624 Locomotion and sleep analysis was run on a 24-hour period, which started at the first onset of
625 light after the flies were placed in the chamber (i.e. 18-24 hours after being placed in the chamber).
626 Locomotion was calculated based on the number of beam crossings over the full 24 hours, the
627 12 hours of light, and the 12 hours of dark. Sleep was classified as 5 minutes without any beam
628 crossings. Total Sleep was quantified as total time spent sleeping over the 12 hours of light and
629 the 12 hours of dark. Sleep latency was quantified as the amount of time after light onset or dark
630 onset before a 5-minute period of sleep. Sleep Bout Length was quantified as the average length
631 of sleep bouts (>5-minute period of sleep) during the 12 hours of light and 12 hours of dark.

632 "Outliers" were classified as lines that were more than two standard deviations from the mean of
633 all lines for any of the phenotypes scored (24-hour locomotion, 12-hour light locomotion, 12-hour
634 dark locomotion, 12-hour light total sleep, 12-hour dark total sleep, 12-hour light sleep bout length,
635 12-hour dark sleep bout length, sleep latency during the light, or sleep latency during the dark).

636 Mask follow up behavior studies

637 For these studies, similar tools and settings were used with these core exceptions. Upon eclosion
638 flies were transferred and kept at 25°C in group housing. For the behavior without drugs, individual
639 males were placed in tubes with sucrose food (2% agar + 5% sucrose) at 3-6 dpe and behavioral
640 analysis was collected and analyzed for the following five days. Sleep was then averaged across
641 the five days for each individual fly before statistical analysis was performed. For the behavior
642 with drugs, similar conditions were followed, except data was collected on the 2-6 days after they
643 were loaded into behavior tubes to allow the drug to take effect. The following drug doses were
644 used for their respective experiments (L-DOPA: 3mg/mL L-DOPA + 12.5 µg/mL carbidopa;
645 caffeine: 0.5 mg/mL caffeine; NACA: 40 µg/mL N-acetylcysteine amide antioxidant). Drugs were
646 dissolved directly into the sucrose food except for carbidopa which was dissolve in H_2O at 1:50x
647 concentration and then added into the sucrose food.

648 # High Performance Liquid Chromatography (HPLC) analysis

649 ## Sample Preparation

650 For the HPLC on fly heads and brain, we adapted and modified the protocol previously published
651 (95,96). Crosses were reared at 29°C and flies were transferred into new tubes 0-2 days post
652 eclosion (dpe). They remained at 29°C until they were 3-5 dpe. Female heads were collected by
653 anesthetizing flies with CO_2 and cutting their heads off with a razor blade. Samples were collected
654 between ZT04-ZT08. The heads were placed into 60 µL of 50 mM citrate acetate (pH=4.5) and
655 either used for analysis that day or frozen at -20°C. Five heads were used per sample, and ~10
656 samples were run per genotype. The day of HPLC analysis, the samples were thawed and
657 grounded using a pestle for 30 seconds (Cordless Pestle Motor and Fisherbrand™ Disposable
658 Pellet Pestle for 1.5mL tube). Then the samples were spun down at 13,000 rpm for 10 minutes.
659 The supernatant was removed and placed into a new vial. 10 µL from each sample was used for
660 the Bradford Protein Analysis Assay. The rest of the sample solution (~40-50 µL) was loaded into
661 a vial (300 µL Polypropylene Sample Vials with 8mm Snap Caps) for HPLC analysis.

662 For HPLC analysis on fly brains, flies were collected 3-7 dpe. Then, 10 fly brains (5 male, 5
663 female) were dissected in ice cold PBS. Right after dissection, the brains were transferred to 60uL
664 of ice cold 50mM citrate acetate (pH=4.5). Samples were frozen at -20°C and ran within 4 weeks
665 of collection. The day of HPLC analysis, the samples were homogenized similarly to the fly heads,
666 though for the Protein Assay, 20 µL of sample was used. Then, the remaining solution was loaded
667 for HPLC analysis.

668 ## Bradford Protein Analysis Assay

669 The Bio-Rad Bradford Assay was used for colorimetric scoring of total protein. See product details
670 for full description (Bio-Rad Protein Assay Kit I #5000001). Briefly, the dye reagent was diluted
671 1:4 in MilliQ H_2O. Then, the solution was filtered through a 0.22 µm SFCA Nalgene filter. 10 µL
672 of each protein sample (standard or fly sample) was placed into single wells of a 96-well plate.
673 Then, 200 µL of diluted 1:4 dye reagent was added to each well. The samples rested for 30-45
674 minutes and then absorbance was measured using BMG Labtech FLUOstar OPTIMA microplate
675 reader. Protein measurements for each sample were calculated based on standards ran on the
676 same plate.

677 **HPLC Information**

678 The HPLC used is an Antec® Scientific product with a LC110S pump, SYSTEC OEM MINI
679 Vacuum Degasser, AS110 autosampler, a SenCell flow cell with salt bridge reference electrode
680 in the Decade Lite. Data was collected and processed using DataApex Clarity™ chromatography
681 software. The column used is chosen to work well for neurotransmitters (Acquity UPLC BEH C18
682 Column, 130Å, 1.7 µm, 1 mm X 100 mm with Acquity In-Line 0.2 µm Filter). The mobile phase
683 was a 6% Acetonitrile mobile phase optimized for our samples (74.4 mg $NA_2EDTA{\cdot}2H_20$, 13.72
684 mL 85% w/v phosphoric acid, 42.04 g citric acid, 1.2 g OSA, 120 mL acetonitrile, H_20 up to 2L,
685 pH=6.0 using 50% NaOH solution). The mobile phase was degassed for 10 minutes using the
686 Bransonic® Ultrasonic Bath before being loaded into the HPLC machine.

687 The standards for HPLC were made by generating master stocks of 100 mM dopamine and 10
688 mM serotonin diluted in MilliQ H_2O, which were kept at 4°C. The day of HPLC analysis, the master
689 stocks were diluted to produce standards ranging from 5-100 nM for 5-HT and 5-1000 nM for
690 dopamine. Sample concentrations of dopamine (Sigma-Aldrich, Cat#H8502) and serotonin
691 (Sigma-Aldrich, Cat#H7752) were calculated based on standards run in the same batch.
692 Standards were compared to standards run on other days to assess for overall performance.

693 # RNA expression analysis

694 Flies were raised at 29°C until 5-7 dpe, then heads were collected by cutting them off with a razor
695 blade. Twenty heads were collected per sample with a mixture of males and females and placed
696 directly on dry ice. Samples were kept on dry ice or at -80°C until RNA isolation. For RNA isolation
697 samples were homogenized in 200µL of TRIzol®. Then 800µL of TRIzol® was added and the
698 samples were mixed by pipetting. The samples incubated for 5 minutes at room temperature and
699 were then spun down at 12,000 rpm for 10 minutes at 4°C. The supernatant was removed and
700 200µL of chloroform was added. The samples were mixed by shaking and then incubated at room
701 temperature for 3 minutes. Then, they were spun at 10,000 rpm for 15 minutes at 4°C, and the
702 aqueous layer was collected and placed in a new tube. 500µL of isopropanol was added and the
703 samples were left to incubate for 10 minutes at room temperature. The samples were spun at
704 10,000 rpm for 10 minutes at 4°C and the supernatant was removed. The pellet was washed with
705 1mL of 75% EtOH and centrifuged at 5,000 rpm for 5 minutes. All EtOH was removed and the
706 pellet dried at room temperature for 10 minutes. Then, the pellet was dissolved in 100µL of H_2O.
707 RNA content and quality was measured using DeNovix DS-11 Fx spectrophotometer/fluorometer.
708 cDNA reverse transcription was performed according to the iScript™ reverse transcriptase Bio-
709 Rad kit and 2 µL of RNA sample was added in a 10 µL reaction for both the reverse and no
710 reverse transcriptase reaction. Samples were measured for content and quality and then they
711 were diluted to 100ng/µL. qPCR was performed using Bio-Rad iQ SYBR Green Supermix and
712 measured on Bio-Rad CFX96™ Real-Time System. The TH primers used Forward: 5'-
713 ATGTTCGCCATCAAGAAATCCT-3' and Reverse: 5'-GGGTCTCGAAACGGGCATC-3', and the
714 control primers were for Rpl32 were Forward: 5'-ATGCTAAGCTGTCGCACAAATG-3' and
715 Reverse: 5'-GTTCGATCCGTAACCGATGT-3'. For each sample, two technical replicates were
716 run for the reverse transcriptase reaction, and the final quantity was based on the average of the

717 two. If the no reverse transcriptase reaction produced a product that was a Cq within ten, the
718 sample was discarded.

719 DAN and TH Quantification

720 Samples were stained and imaged like the brain expression analysis, except the primarily
721 antibody solution included an Elav antibody [anti-Tyrosine Hydroxylase 1:500, PelFreez
722 Biologicals, rabbit, P40101; anti-Elav 1:100, Developmental Studies Hybridoma Bank, rat,
723 7E8A10 in solution (5% Normal Donkey Serum, 0.1% NaN_3 in 0.5% PBST)]. Confocal imaging
724 was performed as described above. Once the samples were imaged, anterior, posterior, and
725 whole brain projections were generated that included all fluorescent signals from the anterior (PAL
726 and PAM clusters) and posterior (PPL1, PPM2, PPM3, PPL2ab) neuron clusters of interest. The
727 number of neurons per cluster (excluding the PAM cluster) were counted for each sample. PPM2
728 and PPM3 clusters were counted together. For TH protein quantification samples were assessed
729 using ImageJ. A boundary was drawn around each individual cluster and quantified. Then, the
730 local background for that cluster was subtracted from the cluster to give the fluorescence for the
731 given sample. Each hemisphere was treated as a separate sample.

732 Statistical Analysis

733 Statistical analysis was performed using Graphpad Prism 10. Unless otherwise stated, all data
734 was subjected to a ROUT outlier test, where all outliers were removed, and then a one-way
735 ANOVA was performed. Each of the experimental samples were compared to the control for the
736 given samples. In the cases where there were only two samples (i.e. control and experimental),
737 a t-test was performed.

738 For the HPLC screen on heads, the samples were normalized to the controls run on that day. The
739 TRiP collection was normalized to *UAS-mCh RNAi* control and the NIG collection was normalized
740 to the *UAS-lacZ RNAi* control.

741 References

742 1. Radwan B, Liu H, Chaudhury D. The role of dopamine in mood disorders and the
743 associated changes in circadian rhythms and sleep-wake cycle. Brain Res [Internet].
744 2019 Jan;1713:42–51. Available from: https://pubmed.ncbi.nlm.nih.gov/30481503/
745 2. Grace AA. Dysregulation of the dopamine system in the pathophysiology of
746 schizophrenia and depression. Nat Rev Neurosci [Internet]. 2016 Jan;17(8):524–32.
747 Available from: https://pubmed.ncbi.nlm.nih.gov/27256556/
748 3. Nutt DJ, Lingford-Hughes A, Erritzoe D, Stokes PRA. The dopamine theory of addiction:
749 40 years of highs and lows. Nat Rev Neurosci [Internet]. 2015 Jan;16(5):305–12.
750 Available from: https://pubmed.ncbi.nlm.nih.gov/25873042/
751 4. Church FC. Treatment Options for Motor and Non-Motor Symptoms of Parkinson's
752 Disease. Biomolecules [Internet]. 2021 Jan;11(4). Available from:
753 https://pubmed.ncbi.nlm.nih.gov/33924103/
754 5. Armstrong MJ, Okun MS. Diagnosis and Treatment of Parkinson Disease: A Review.
755 JAMA [Internet]. 2020 Jan;323(6):548–60. Available from:
756 https://pubmed.ncbi.nlm.nih.gov/32044947/
757 6. López-Cruz L, Miguel NS, Carratalá-Ros C, Monferrer L, Salamone JD, Correa M.
758 Dopamine depletion shifts behavior from activity based reinforcers to more sedentary
759 ones and adenosine receptor antagonism reverses that shift: Relation to ventral striatum
760 DARPP32 phosphorylation patterns. Neuropharmacology [Internet]. 2018 Jan;138:349–
761 59. Available from: https://pubmed.ncbi.nlm.nih.gov/29408363/

762 7. Steiner H, Kitai ST. Unilateral striatal dopamine depletion: time-dependent effects on
763 cortical function and behavioural correlates. Eur J Neurosci [Internet]. 2001;14(8):1390–
764 404. Available from: https://pubmed.ncbi.nlm.nih.gov/11703467/
765 8. Rohwedder A, Wenz NL, Stehle B, Huser A, Yamagata N, Zlatic M, et al. Four
766 Individually Identified Paired Dopamine Neurons Signal Reward in Larval Drosophila.
767 Curr Biol [Internet]. 2016 Jan;26(5):661–9. Available from:
768 https://pubmed.ncbi.nlm.nih.gov/26877086/
769 9. Budnik V, White K. Genetic dissection of dopamine and serotonin synthesis in the
770 nervous system of Drosophila melanogaster. J Neurogenet [Internet]. 1987 Jan;4(6):309–
771 14. Available from: https://www.tandfonline.com/doi/abs/10.3109/01677068709167191
772 10. Livingstone MS, Tempel BL. Genetic dissection of monoamine neurotransmitter synthesis
773 in Drosophila. Nature [Internet]. 1983;303(5912):67–70. Available from:
774 https://pubmed.ncbi.nlm.nih.gov/6133219/
775 11. Meiser J, Weindl D, Hiller K. Complexity of dopamine metabolism. Cell Commun Signal
776 [Internet]. 2013;11(1). Available from: https://pubmed.ncbi.nlm.nih.gov/23683503/
777 12. Yamamoto S, Seto ES. Dopamine dynamics and signaling in Drosophila: an overview of
778 genes, drugs and behavioral paradigms. Exp Anim [Internet]. 2014;63(2):107–19.
779 Available from: https://pubmed.ncbi.nlm.nih.gov/24770636/
780 13. Wittkopp PJ, True JR, Carroll SB. Reciprocal functions of the Drosophila yellow and
781 ebony proteins in the development and evolution of pigment patterns. Development
782 [Internet]. 2002;129(8):1849–58. Available from:
783 https://pubmed.ncbi.nlm.nih.gov/11934851/
784 14. True JR, Edwards KA, Yamamoto D, Carroll SB. Drosophila wing melanin patterns form
785 by vein-dependent elaboration of enzymatic prepatterns. Curr Biol [Internet]. 1999
786 Jan;9(23):1382–91. Available from: https://pubmed.ncbi.nlm.nih.gov/10607562/

787 15. Spana EP, Abrams AB, Ellis KT, Klein JC, Ruderman BT, Shi AH, et al. speck, First
788 Identified in Drosophila melanogaster in 1910, Is Encoded by the Arylalkalamine N-
789 Acetyltransferase (AANAT1) Gene. G3 (Bethesda) [Internet]. 2020 Jan;10(9):3387–98.
790 Available from: https://pubmed.ncbi.nlm.nih.gov/32709620/
791 16. Gervasi N, Tchénio P, Preat T. PKA dynamics in a Drosophila learning center:
792 coincidence detection by rutabaga adenylyl cyclase and spatial regulation by dunce
793 phosphodiesterase. Neuron [Internet]. 2010 Jan;65(4):516–29. Available from:
794 https://pubmed.ncbi.nlm.nih.gov/20188656/
795 17. Heisenberg M, Borst A, Wagner S, Byers D. Drosophila mushroom body mutants are
796 deficient in olfactory learning. J Neurogenet [Internet]. 1985;2(1):1–30. Available from:
797 https://pubmed.ncbi.nlm.nih.gov/4020527/
798 18. Jenett A, Rubin GM, Ngo TTB, Shepherd D, Murphy C, Dionne H, et al. A GAL4-driver
799 line resource for Drosophila neurobiology. Cell Rep [Internet]. 2012 Jan;2(4):991–1001.
800 Available from: https://pubmed.ncbi.nlm.nih.gov/23063364/
801 19. Frighetto G, Zordan MA, Castiello U, Megighian A, Martin JR. Dopamine Modulation of
802 Drosophila Ellipsoid Body Neurons, a Nod to the Mammalian Basal Ganglia. Front
803 Physiol [Internet]. 2022 Jan;13. Available from:
804 https://pubmed.ncbi.nlm.nih.gov/35492587/
805 20. Xie T, Ho MCW, Liu Q, Horiuchi W, Lin CC, Task D, et al. A Genetic Toolkit for Dissecting
806 Dopamine Circuit Function in Drosophila. Cell Rep. 2018 Apr 10;23(2):652–65.
807 21. Clark IE, Dodson MW, Jiang C, Cao JH, Huh JR, Seol JH, et al. Drosophila pink1 is
808 required for mitochondrial function and interacts genetically with parkin. Nature [Internet].
809 2006 Jan;441(7097):1162–6. Available from: https://pubmed.ncbi.nlm.nih.gov/16672981/
810 22. Mummery-Widmer JL, Yamazaki M, Stoeger T, Novatchkova M, Bhalerao S, Chen D, et
811 al. Genome-wide analysis of Notch signalling in Drosophila by transgenic RNAi. Nature

812 [Internet]. 2009 Jan;458(7241):987–92. Available from:
813 https://pubmed.ncbi.nlm.nih.gov/19363474/
814 23. Pendleton RG, Rasheed A, Sardina T, Tully T, Hillman R. Effects of Tyrosine
815 Hydroxylase Mutants on Locomotor Activity in Drosophila: A Study in Functional
816 Genomics. Vol. 32, Behavior Genetics. 2002.
817 24. Wright TRF, Bewleyz GC, Sherald3 AF. THE GENETICS OF DOPA DECARBOXYLASE
818 IN DROSOPHILA MELANOGASTER. 11. ISOLATION AND CHARACTERIZATION OF
819 DOPA-DECARBOXY LASE-DEFICIENT MUTANTS AND THEIR RELATIONSHIP TO
820 THE a-METHYL-DOPA-HYPERSENSITIVE MUTANTS. Vol. 8, Genetics. 1976.
821 25. Ni JQ, Liu LP, Binari R, Hardy R, Shim HS, Cavallaro A, et al. A Drosophila resource of
822 transgenic RNAi lines for neurogenetics. Genetics [Internet]. 2009 Jan;182(4):1089–100.
823 Available from: https://pubmed.ncbi.nlm.nih.gov/19487563/
824 26. Pan Y, Li W, Deng Z, Sun Y, Ma X, Liang R, et al. Myc suppresses male-male courtship
825 in Drosophila. EMBO J [Internet]. 2022 Jan;41(7). Available from:
826 https://pubmed.ncbi.nlm.nih.gov/35167135/
827 27. Riemensperger T, Issa AR, Pech U, Coulom H, Nguyễn MV, Cassar M, et al. A single
828 dopamine pathway underlies progressive locomotor deficits in a Drosophila model of
829 Parkinson disease. Cell Rep [Internet]. 2013 Jan;5(4):952–60. Available from:
830 https://pubmed.ncbi.nlm.nih.gov/24239353/
831 28. Brand H, Perrimon N. Targeted gene expression as a means of altering cell fates and
832 generating dominant phenotypes. 1993.
833 29. Bayersdorfer F, Voigt A, Schneuwly S, Botella JA. Dopamine-dependent
834 neurodegeneration in Drosophila models of familial and sporadic Parkinson's disease.
835 Neurobiol Dis [Internet]. 2010 Jan;40(1):113–9. Available from:
836 https://pubmed.ncbi.nlm.nih.gov/20211259/

837 30. Hovemann BT, Ryseck RP, Walldorf U, Störtkuhl KF, Dietzel ID, Dessen E. The
838 Drosophila ebony gene is closely related to microbial peptide synthetases and shows
839 specific cuticle and nervous system expression. Gene [Internet]. 1998 Jan;221(1):1–9.
840 Available from: https://pubmed.ncbi.nlm.nih.gov/9852943/
841 31. Richardt A, Rybak J, Störtkuhl KF, Meinertzhagen IA, Hovemann BT. Ebony protein in
842 the Drosophila nervous system: optic neuropile expression in glial cells. J Comp Neurol
843 [Internet]. 2002 Jan;452(1):93–102. Available from:
844 https://pubmed.ncbi.nlm.nih.gov/12205712/
845 32. Yamamoto-Hino M, Yoshida H, Ichimiya T, Sakamura S, Maeda M, Kimura Y, et al.
846 Phenotype-based clustering of glycosylation-related genes by RNAi-mediated gene
847 silencing. Genes to Cells. 2015 Jun 1;20(6):521–42.
848 33. Riemensperger T, Isabel G, Coulom H, Neuser K, Seugnet L, Kume K, et al. Behavioral
849 consequences of dopamine deficiency in the Drosophila central nervous system. Proc
850 Natl Acad Sci U S A. 2011 Jan;108(2):834–9.
851 34. Chiu JC, Low KH, Pike DH, Yildirim E, Edery I. Assaying locomotor activity to study
852 circadian rhythms and sleep parameters in Drosophila. Journal of Visualized
853 Experiments. 2010;(43).
854 35. Dietzl G, Chen D, Schnorrer F, Su KC, Barinova Y, Fellner M, et al. A genome-wide
855 transgenic RNAi library for conditional gene inactivation in Drosophila. Nature [Internet].
856 2007 Jan;448(7150):151–6. Available from: https://pubmed.ncbi.nlm.nih.gov/17625558/
857 36. Ni JQ, Zhou R, Czech B, Liu LP, Holderbaum L, Yang-Zhou D, et al. A genome-scale
858 shRNA resource for transgenic RNAi in Drosophila. Nat Methods [Internet]. 2011
859 Jan;8(5):405–7. Available from: https://pubmed.ncbi.nlm.nih.gov/21460824/
860 37. Vissers JHA, Manning SA, Kulkarni A, Harvey KF. A Drosophila RNAi library modulates
861 Hippo pathway-dependent tissue growth. Nature Communications 2016 7:1 [Internet].
862 2016 Jan;7(1):1–6. Available from: https://www.nature.com/articles/ncomms10368

863 38. Shafer OT, Keene AC. The Regulation of Drosophila Sleep. Vol. 31, Current Biology. Cell
864 Press; 2021. p. R38–49.
865 39. Diao F, Ironfield H, Luan H, Diao F, Shropshire WC, Ewer J, et al. Plug-and-play genetic
866 access to drosophila cell types using exchangeable exon cassettes. Cell Rep [Internet].
867 2015 Jan;10(8):1410–21. Available from: https://pubmed.ncbi.nlm.nih.gov/25732830/
868 40. Lee PT, Zirin J, Kanca O, Lin WW, Schulze KL, Li-Kroeger D, et al. A gene-specific T2A-
869 GAL4 library for Drosophila. Elife [Internet]. 2018 Jan;7. Available from:
870 https://pubmed.ncbi.nlm.nih.gov/29565247/
871 41. Kanca O, Zirin J, Garcia-Marques J, Knight SM, Yang-Zhou D, Amador G, et al. An
872 efficient CRISPR-based strategy to insert small and large fragments of DNA using short
873 homology arms. VijayRaghavan K, VijayRaghavan K, editors. Elife [Internet]. 2019
874 Nov;8:e51539. Available from: https://doi.org/10.7554/eLife.51539
875 42. Janssens J, Aibar S, Taskiran II, Ismail JN, Gomez AE, Aughey G, et al. Decoding gene
876 regulation in the fly brain. Nature [Internet]. 2022 Jan;601(7894):630–6. Available from:
877 https://pubmed.ncbi.nlm.nih.gov/34987221/
878 43. Li H, Janssens J, de Waegeneer M, Kolluru SS, Davie K, Gardeux V, et al. Fly Cell Atlas:
879 A single-nucleus transcriptomic atlas of the adult fruit fly. Science (1979). 2022 Mar
880 4;375(6584).
881 44. Mao Z, Davis RL. Eight different types of dopaminergic neurons innervate the Drosophila
882 mushroom body neuropil: Anatomical and physiological heterogeneity. Front Neural
883 Circuits. 2009 Jan;3(JUL):5.
884 45. Morin X, Daneman R, Zavortink M, Chia W. A protein trap strategy to detect GFP-tagged
885 proteins expressed from their endogenous loci in Drosophila [Internet]. Available from:
886 www.pnas.orgcgidoi10.1073pnas.261408198

887 46. Buszczak M, Paterno S, Lighthouse D, Bachman J, Planck J, Owen S, et al. The
888 carnegie protein trap library: A versatile tool for drosophila developmental studies.
889 Genetics. 2007 Mar;175(3):1505–31.
890 47. Voet M Van Der, Harich B, Franke B, Schenck A. ADHD-associated dopamine
891 transporter, latrophilin and neurofibromin share a dopamine-related locomotor signature
892 in Drosophila. Mol Psychiatry. 2016 Jan;21(4):565–73.
893 48. Kume K, Kume S, Park SK, Hirsh J, Jackson FR. Dopamine is a regulator of arousal in
894 the fruit fly. Journal of Neuroscience. 2005 Jan;25(32):7377–84.
895 49. Nall AH, Shakhmantsir I, Cichewicz K, Birman S, Hirsh J, Sehgal A. Caffeine promotes
896 wakefulness via dopamine signaling in Drosophila. Sci Rep. 2016 Jan;6.
897 50. Ni JQ, Markstein M, Binari R, Pfeiffer B, Liu LP, Villalta C, et al. Vector and parameters
898 for targeted transgenic RNA interference in Drosophila melanogaster. Nature Methods
899 2008 5:1 [Internet]. 2007 Jan;5(1):49–51. Available from:
900 https://www.nature.com/articles/nmeth1146
901 51. McGary KL, Park TJ, Woods JO, Cha HJ, Wallingford JB, Marcotte EM. Systematic
902 discovery of nonobvious human disease models through orthologous phenotypes. Proc
903 Natl Acad Sci U S A. 2010 Apr 6;107(14):6544–9.
904 52. Nakashima A, Ohnuma S, Kodani Y, Kaneko YS, Nagasaki H, Nagatsu T, et al. Inhibition
905 of deubiquitinating activity of USP14 decreases tyrosine hydroxylase phosphorylated at
906 Ser19 in PC12D cells. Biochem Biophys Res Commun [Internet]. 2016 Jan;472(4):598–
907 602. Available from: https://pubmed.ncbi.nlm.nih.gov/26969276/
908 53. Kawahata I, Ohtaku S, Tomioka Y, Ichinose H, Yamakuni T. Dopamine or biopterin
909 deficiency potentiates phosphorylation at (40)Ser and ubiquitination of tyrosine
910 hydroxylase to be degraded by the ubiquitin proteasome system. Biochem Biophys Res
911 Commun [Internet]. 2015 Jan;465(1):53–8. Available from:
912 https://pubmed.ncbi.nlm.nih.gov/26225746/

913 54. Birman S, Morgan B, Anzivino M, Hirsh J. A novel and major isoform of tyrosine
914 hydroxylase in Drosophila is generated by alternative RNA processing. Journal of
915 Biological Chemistry. 1994 Jan;269(42):26559–67.
916 55. Vié A, Cigna M, Toci R, Birman S. Differential regulation of Drosophila tyrosine
917 hydroxylase isoforms by dopamine binding and cAMP-dependent phosphorylation. J Biol
918 Chem [Internet]. 1999 Jan;274(24):16788–95. Available from:
919 https://pubmed.ncbi.nlm.nih.gov/10358021/
920 56. Gervasi NM, Scott SS, Aschrafi A, Gale J, Vohra SN, Macgibeny MA, et al. The local
921 expression and trafficking of tyrosine hydroxylase mRNA in the axons of sympathetic
922 neurons. RNA [Internet]. 2016 Jan;22(6):883–95. Available from:
923 https://pubmed.ncbi.nlm.nih.gov/27095027/
924 57. Freeman A, Pranski E, Miller RD, Radmard S, Bernhard D, Jinnah HA, et al. Sleep
925 fragmentation and motor restlessness in a Drosophila model of Restless Legs Syndrome.
926 Current Biology [Internet]. 2012 Jan;22(12):1142. Available from:
927 /pmc/articles/PMC3381864/
928 58. Chaudhuri A, Bowling K, Funderburk C, Lawal H, Inamdar A, Wang Z, et al. Interaction of
929 Genetic and Environmental Factors in a Drosophila Parkinsonism Model. The Journal of
930 Neuroscience [Internet]. 2007 Jan;27(10):2457. Available from:
931 /pmc/articles/PMC6672491/
932 59. Wang Z, Ferdousy F, Lawal H, Huang Z, Daigle JG, Izevbaye I, et al. Catecholamines up
933 integrates dopamine synthesis and synaptic trafficking. J Neurochem [Internet]. 2011
934 Jan;119(6):1294–305. Available from: https://pubmed.ncbi.nlm.nih.gov/21985068/
935 60. Zhang YQ, Friedman DB, Wang Z, Woodruff E, Pan L, O'Donnell J, et al. Protein
936 expression profiling of the Drosophila fragile X mutant brain reveals up-regulation of
937 monoamine synthesis. Molecular and Cellular Proteomics [Internet]. 2005 Jan;4(3):278–
938 90. Available from: http://www.mcponline.org/article/S1535947620326864/fulltext

939 61. Wicker-Thomas C, Hamann M. Interaction of dopamine, female pheromones, locomotion
940 and sex behavior in Drosophila melanogaster. J Insect Physiol. 2008 Oct;54(10–
941 11):1423–31.
942 62. Takahashi A. Pigmentation and behavior: potential association through pleiotropic genes
943 in Drosophila. Vol. 88, Genes Genet. Syst. 2013.
944 63. Letizia A, Bario R, Campuzano S. Antagonistic and cooperative actions of the EGFR and
945 Dpp pathways on the iroquois genes regulate Drosophila mesothorax specification and
946 patterning. Development [Internet]. 2007 Jan;134(7):1337–46. Available from:
947 https://pubmed.ncbi.nlm.nih.gov/17329358/
948 64. Lu J, Wang Y, Wang X, Wang D, Pflugfelder GO, Shen J. The Tbx6 Transcription Factor
949 Dorsocross Mediates Dpp Signaling to Regulate Drosophila Thorax Closure. Int J Mol Sci
950 [Internet]. 2022 Jan;23(9). Available from: https://pubmed.ncbi.nlm.nih.gov/35562934/
951 65. Zeitlinger J, Bohmann D. Thorax closure in Drosophila: involvement of Fos and the JNK
952 pathway. Development [Internet]. 1999 Jan;126(17):3947–56. Available from:
953 https://pubmed.ncbi.nlm.nih.gov/10433922/
954 66. Massey JH, Akiyama N, Bien T, Dreisewerd K, Wittkopp PJ, Yew JY, et al. Pleiotropic
955 Effects of ebony and tan on Pigmentation and Cuticular Hydrocarbon Composition in
956 Drosophila melanogaster. Front Physiol. 2019 Jan;10(MAY):518.
957 67. Zhang S, Wang R, Wang G. Impact of Dopamine Oxidation on Dopaminergic
958 Neurodegeneration. ACS Chem Neurosci [Internet]. 2019 Jan;10(2):945–53. Available
959 from: https://pubs.acs.org/doi/abs/10.1021/acschemneuro.8b00454
960 68. Davla S, Artiushin G, Li Y, Chitsaz D, Li S, Sehgal A, et al. AANAT1 functions in
961 astrocytes to regulate sleep homeostasis. Elife [Internet]. 2020 Jan;9:1–48. Available
962 from: https://pubmed.ncbi.nlm.nih.gov/32955431/

963 69. DeAngelis MW, McGhie EW, Coolon JD, Johnson RI. Mask, a component of the Hippo
964 pathway, is required for Drosophila eye morphogenesis. Dev Biol. 2020 Aug 1;464(1):53–
965 70.
966 70. Zhu M, Zhang S, Tian X, Wu C. Mask mitigates MAPT- and FUS-induced degeneration
967 by enhancing autophagy through lysosomal acidification. Autophagy. 2017 Nov
968 2;13(11):1924–38.
969 71. Martinez D, Zhu M, Guidry JJ, Majeste N, Mao H, Yanofsky ST, et al. Mask, the
970 Drosophila ankyrin repeat and KH domain-containing protein, affects microtubule stability.
971 J Cell Sci. 2021 Oct 1;134(20).
972 72. Dubowy C, Sehgal A. Circadian rhythms and sleep in Drosophila melanogaster.
973 Genetics. 2017 Jan;205(4):1373–97.
974 73. Sidor CM, Brain R, Thompson BJ. Mask proteins are cofactors of Yorkie/YAP in the
975 Hippo pathway. Curr Biol [Internet]. 2013 Jan;23(3):223–8. Available from:
976 https://pubmed.ncbi.nlm.nih.gov/23333315/
977 74. Sansores-Garcia L, Atkins M, Moya IM, Shahmoradgoli M, Tao C, Mills GB, et al. Mask is
978 required for the activity of the Hippo pathway effector Yki/YAP. Curr Biol [Internet]. 2013
979 Jan;23(3):229–35. Available from: https://pubmed.ncbi.nlm.nih.gov/23333314/
980 75. Smith RK, Carroll PM, Allard JD, Simon MA. MASK, a large ankyrin repeat and KH
981 domain-containing protein involved in Drosophila receptor tyrosine kinase signaling.
982 Development [Internet]. 2002;129(1):71–82. Available from:
983 https://pubmed.ncbi.nlm.nih.gov/11782402/
984 76. Zhu M, Li X, Tian X, Wu C. Mask loss-of-function rescues mitochondrial impairment and
985 muscle degeneration of Drosophila pink1 and parkin mutants. Hum Mol Genet [Internet].
986 2015 Jan;24(11):3272–85. Available from: https://pubmed.ncbi.nlm.nih.gov/25743185/

987 77. Lusk JB, Lam VYM, Tolwinski NS. Epidermal Growth Factor Pathway Signaling in
988 Drosophila Embryogenesis: Tools for Understanding Cancer. Cancers (Basel) [Internet].
989 2017 Jan;9(2). Available from: /pmc/articles/PMC5332939/
990 78. Oh H, Irvine KD. Yorkie: the final destination of Hippo signaling. Trends Cell Biol
991 [Internet]. 2010 Jan;20(7):410. Available from: /pmc/articles/PMC2919348/
992 79. Sen A, Kalvakuri S, Bodmer R, Cox RT. Clueless, a protein required for mitochondrial
993 function, interacts with the PINK1-Parkin complex in Drosophila. Dis Model Mech
994 [Internet]. 2015 Jan;8(6):577–89. Available from:
995 https://pubmed.ncbi.nlm.nih.gov/26035866/
996 80. Wang ZH, Clark C, Geisbrecht ER. Drosophila clueless is involved in Parkin-dependent
997 mitophagy by promoting VCP-mediated Marf degradation. Hum Mol Genet [Internet].
998 2016 Jan;25(10):1946–64. Available from: https://pubmed.ncbi.nlm.nih.gov/26931463/
999 81. Sen A, Cox RT. Clueless is a conserved ribonucleoprotein that binds the ribosome at the
1000 mitochondrial outer membrane. Biol Open [Internet]. 2016 Jan;5(2):195–203. Available
1001 from: https://pubmed.ncbi.nlm.nih.gov/26834020/
1002 82. Inagaki HK, De-Leon SBT, Wong AM, Jagadish S, Ishimoto H, Barnea G, et al.
1003 Visualizing Neuromodulation In Vivo: TANGO-Mapping of Dopamine Signaling Reveals
1004 Appeptite Control of Sugar Sensing. Cell [Internet]. 2012 Jan;148(3):583. Available from:
1005 /pmc/articles/PMC3295637/
1006 83. Sun F, Zhou J, Dai B, Qian T, Zeng J, Li X, et al. Next-generation GRAB sensors for
1007 monitoring dopaminergic activity in vivo. Nat Methods [Internet]. 2020 Jan;17(11):1156.
1008 Available from: /pmc/articles/PMC7648260/
1009 84. Kasture AS, Hummel T, Sucic S, Freissmuth M. Big Lessons from Tiny Flies: Drosophila
1010 melanogaster as a Model to Explore Dysfunction of Dopaminergic and Serotonergic
1011 Neurotransmitter Systems. Int J Mol Sci [Internet]. 2018 Jan;19(6). Available from:
1012 https://pubmed.ncbi.nlm.nih.gov/29914172/

1013 85. Calleja M, Herranz H, Estella C, Casal J, Lawrence P, Simpson P, et al. Generation of
1014 medial and lateral dorsal body domains by the pannier gene of Drosophila. Development
1015 [Internet]. 2000;127(18):3971–80. Available from:
1016 https://pubmed.ncbi.nlm.nih.gov/10952895/
1017 86. Kennerdell JR, Carthew RW. Heritable gene silencing in Drosophila using double-
1018 stranded RNA. Nat Biotechnol [Internet]. 2000;18(8):896–8. Available from:
1019 https://pubmed.ncbi.nlm.nih.gov/10932163/
1020 87. Yamamoto S, Charng WL, Rana NA, Kakuda S, Jaiswal M, Bayat V, et al. A mutation in
1021 EGF repeat-8 of notch discriminates between serrate/jagged and delta family ligands.
1022 Science (1979). 2012 Nov 30;338(6111):1229–32.
1023 88. Marcogliese PC, Deal SL, Andrews J, Harnish JM, Bhavana VH, Graves HK, et al.
1024 Drosophila functional screening of de novo variants in autism uncovers damaging
1025 variants and facilitates discovery of rare neurodevelopmental diseases. Cell Rep. 2022
1026 Mar 15;38(11).
1027 89. Snel B, Lehmann G, Bork P, Huynen MA. STRING: a web-server to retrieve and display
1028 the repeatedly occurring neighbourhood of a gene [Internet]. Vol. 28, Nucleic Acids
1029 Research. 2000. Available from: http://www.bork.embl-heidelberg.de/STRING
1030 90. Szklarczyk D, Gable AL, Nastou KC, Lyon D, Kirsch R, Pyysalo S, et al. The STRING
1031 database in 2021: Customizable protein-protein networks, and functional characterization
1032 of user-uploaded gene/measurement sets. Nucleic Acids Res. 2021 Jan 8;49(D1):D605–
1033 12.
1034 91. Szklarczyk D, Kirsch R, Koutrouli M, Nastou K, Mehryary F, Hachilif R, et al. The STRING
1035 database in 2023: protein-protein association networks and functional enrichment
1036 analyses for any sequenced genome of interest. Nucleic Acids Res. 2023 Jan 6;51(1
1037 D):D638–46.

1038 92. Hu Y, Flockhart I, Vinayagam A, Bergwitz C, Berger B, Perrimon N, et al. An integrative
1039 approach to ortholog prediction for disease-focused and other functional studies. BMC
1040 Bioinformatics. 2011 Aug 31;12.
1041 93. Hamosh A, Amberger JS, Bocchini C, Scott AF, Rasmussen SA. Online Mendelian
1042 Inheritance in Man (OMIM®): Victor McKusick's magnum opus. Am J Med Genet A. 2021
1043 Nov 1;185(11):3259–65.
1044 94. Abrahams BS, Arking DE, Campbell DB, Mefford HC, Morrow EM, Weiss LA, et al.
1045 SFARI Gene 2.0: A community-driven knowledgebase for the autism spectrum disorders
1046 (ASDs). Mol Autism. 2013;4(1).
1047 95. Cichewicz K, Garren EJ, Adiele C, Aso Y, Wang Z, Wu M, et al. A new brain dopamine-
1048 deficient Drosophila and its pharmacological and genetic rescue. Genes Brain Behav.
1049 2017 Mar 1;16(3):394–403.
1050 96. Hardie SL, Hirsh J. An improved method for the separation and detection of biogenic
1051 amines in adult Drosophila brain extracts by high performance liquid chromatography. J
1052 Neurosci Methods. 2006 Jun 15;153(2):243–9.
1053

1054 Supplemental Information

1055 Document S1. Figures S1-S10

1056 Table S2. Excel file containing data too large to fit in a PDF Table S1-S5

1057

1058 **S1 Fig. GO term enrichment analysis performed on the pigmentation screen hits.**

1059 **S2 Fig. Comparison between genes identified as hits from our pigmentation screen to**
1060 **those tested in the original thorax screen (Mummery-Widmer et al., 2009).**

1061 **S3 Fig. Comparison of dopamine levels between lacZ RNAi and mCh RNAi lines in the fly**
1062 **head.**

1063 **S4 Fig. Validation of recombined GAL4 lines used for dopamine measurement in the brain.**

1064 **S5 Fig. Brain data for prioritized genes with no change in brain dopamine.**

1065 **S6 Fig. Additional clusters of TH positive neurons upon *mask* knockdown show trend or**
1066 **little effect.**

1067 **S7 Fig. Sleep behavior analysis upon TH GAL4 driven TH knockdown.**

1068 **S8 Fig. Additional sleep analysis from TH-GAL4 driven *mask* knockdown.** (

1069 **S9 Fig. Sleep behavior analysis of *clueless* knockdown highlights a different pathway**
1070 **than mask.**

1071 **S10 Fig. Comparison of RNAi lines from the pigmentation screen**

1072 **S11 Fig. Expression analysis for other prioritized candidate genes that did not show any**
1073 **significant change in total head dopamine**.

1074 **S1 Table. Pigmentation screen results by RNAi line**

1075 **S2 Table. Drosophila Activity Monitor results by RNAi line**

1076 **S3 Table. HPLC results by RNAi line**

1077 **S4 Table. Prioritized gene list for HPLC**

1078 **S5 Table. All RNAi lines used with stock center information**